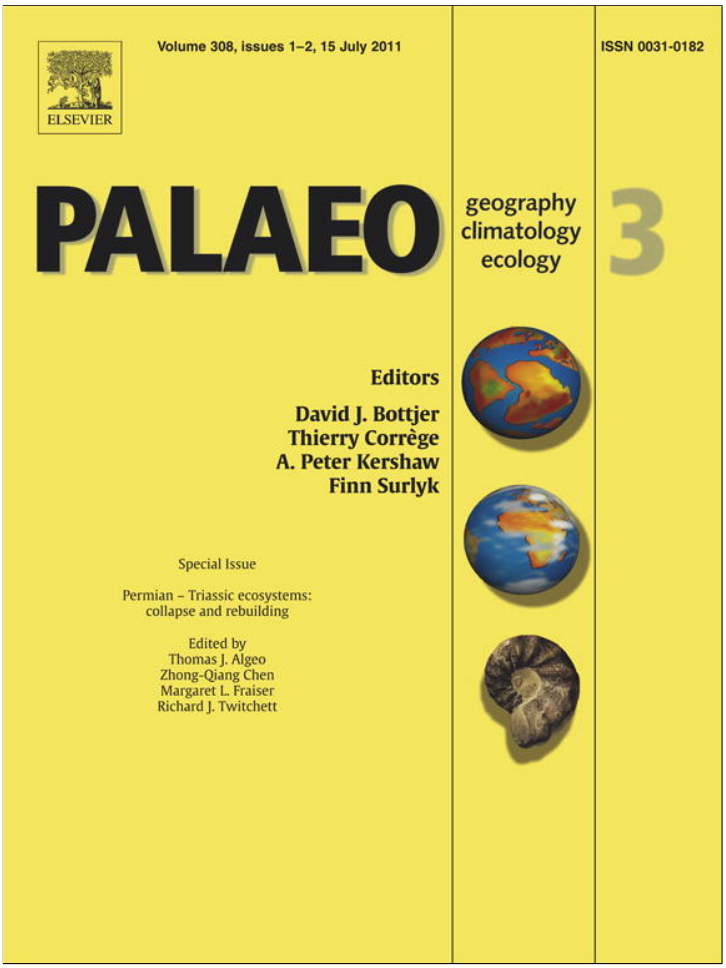

Palaeogeography, Palaeoclimatology, Palaeoecology 308 (2011) 233–251

Contents lists available at ScienceDirect

Palaeogeography, Palaeoclimatology, Palaeoecology

journal homepage: www.elsevier.com/locate/palaeo

Multiple Early Triassic greenhouse crises impeded recovery from Late Permian mass extinction

Gregory J. Retallack [a,*], Nathan D. Sheldon [b], Paul F. Carr [c], Mark Fanning [d], Caitlyn A. Thompson [a], Megan L. Williams [c], Brian G. Jones [c], Adrian Hutton [c]

[a] Department of Geological Sciences, University of Oregon, Eugene, OR, USA 97403-1272
[b] Department of Geological Sciences, University of Michigan, Ann Arbor, MI, USA 48109-1005
[c] School of Geosciences, University of Wollongong, New South Wale, Australia, 2522
[d] Research School of Earth Sciences, Australian National University, Canberra, ACT, Australia 0200

ARTICLE INFO

Article history:
Received 11 February 2010
Received in revised form 7 September 2010
Accepted 20 September 2010
Available online 25 September 2010

Keywords:
Permian
Triassic
Extinction
Carbon dioxide
Paleosol
Amphibian
Fish
Plant

ABSTRACT

The Late Permian mass extinction was not only the most catastrophic known loss of biodiversity, but was followed by unusually prolonged recovery through the Early Triassic. Opinion has been divided on whether delayed recovery was a legacy of especially profound ecological disruption, or due to additional environmental perturbations. New records from the Sydney Basin in southeastern Australia now reveal five successive Late Permian and Early Triassic spikes of unusually high atmospheric CO_2 and profound chemical weathering. These successive atmospheric CO_2 greenhouse crises coincided with unusually warm and wet paleoclimates for a paleolatitude of 61°S. Successive transient greenhouse crises punctuated long-term, cool, dry, and low-CO_2 conditions, and may account for the persistence of low diversity and small size in Early Triassic plants and animals.

1. Introduction

Plants and animals following the greatest known mass extinction during the Late Permian are distinctive and cosmopolitan. Animals on land were dominated by few taxa of small to medium sized therapsids, especially *Lystrosaurus* (Cosgriff et al., 1982; Benton et al., 2004; Retallack et al., 2003). Plants were mainly lycopsids (*Tomiostrobus* and *Pleuromeia*) and conifers (*Voltzia* and *Voltziopsis*: White, 1986; Retallack, 1995; Visscher et al., 2004). In the sea, small paper clams (*Claraia*) and inarticulate brachiopods (*Lingula*) abounded (Hallam and Wignall, 1997; Fraiser and Bottjer, 2004; Twitchett, 2007). Diversity within biotas, regional biotic differentiation, swamp woodlands, reef corals and bryozoans did not recover to Permian levels until the Middle Triassic (Retallack et al., 1996; Payne et al., 2004; Benton et al., 2004; Weidlich, 2007). Such prolonged recovery is well beyond the millennial tempo of ecological succession, which can often be detected even in ancient sequences (Calder et al., 2006). Prolonged recovery has been attributed to exceptional severity of Late Permian extinctions, which decimated key ecological components such as reefs (Pruss and Bottjer, 2004; Weidlich, 2007). An alternative hypothesis is lingering or recurrent environmental hazards, which frustrated full ecological recovery (Fraiser and Bottjer, 2007; Twitchett, 2007).

These alternatives are here re-examined using multiple proxy records from the Sydney Basin, southeastern Australia (Fig. 1). This is but one of many informative Permian–Triassic boundary sections around the world (Retallack and Krull, 2006; Richoz, 2006; Riccardi et al., 2007). Any succession is theoretically as good as another for understanding global CO_2 greenhouse crises of the past, because atmospheric CO_2 is globally mixed on time scales of 2–10 years (Revelle and Suess, 1957; Levin et al., 1992). The Sydney Basin however, has a thick (4.5 km), Permian to Middle Triassic succession (Figs. 2 and 3) and fossil plants and soils as proxies for atmospheric CO_2 and paleoclimate (Retallack, 1980, 1997a,b, 1999a,b). Furthermore, the Sydney Basin was then at high paleolatitude (Blakey, 2008), and it is at high latitudes where effects of current global warming attributed to rising atmospheric CO_2 are most pronounced (Alley et al., 2007).

The centrepiece of our work is a local record of carbon isotopic composition ($\delta^{13}C$) of organic matter (Fig. 3), supplementing earlier records (Compston, 1960; Philip and Saxby, 1979; Morante, 1996; Birgenheier et al., 2010), as a guide to estimating variations in carbon

* Corresponding author. Tel.: +1 541 3464558; fax: +1 541 3464692.
E-mail address: gregr@uoregon.edu (G.J. Retallack).

0031-0182/$ – see front matter © 2010 Elsevier B.V. All rights reserved.
doi:10.1016/j.palaeo.2010.09.022

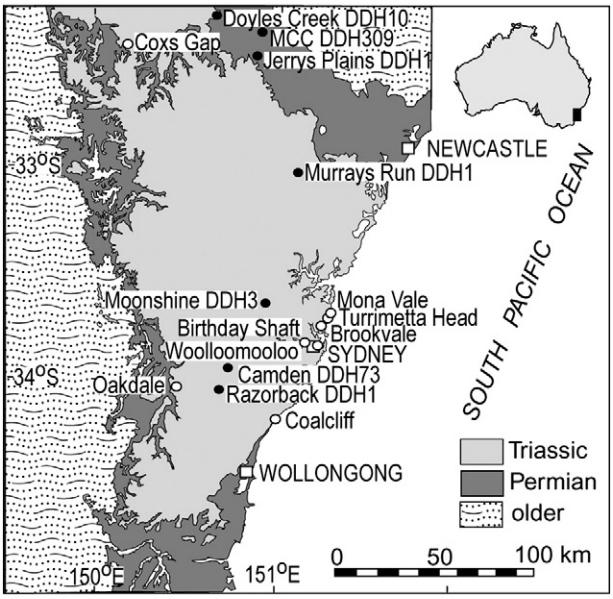

Fig. 1. Geological map of Permian and Triassic rocks of the Sydney Basin, Australia (simplified after Mayne et al., 1974). Localities shown are drillhole cores used for carbon isotope analysis (closed symbols), and localities for fossil plants used for stomatal index studies (open symbols).

sequestration and burial (Jahren et al., 2001), and as a tool for assessing international correlation of the greenhouse crises (Retallack et al., 2006). These new isotopic data complement newly compiled paleoclimatic data of comparable temporal resolution: (1), diversity of spores of lycopsids, which were plants of tropical affinities within these temperate floras (Retallack et al., 2006); (2), measurements of plant leafy shoot size as guides to incursions of frost-sensitive plants (Greenwood and Wing, 1995), and (3), chemical weathering indices of paleosols as guides to mean annual precipitation and temperature (Sheldon and Tabor, 2009). Only five of nine paleoclimatic perturbations identified by these proxies are supported by new estimates from stomatal index of Late Permian and Early Triassic atmospheric CO_2 levels, in support of comparable data from elsewhere in the world (Retallack, 2001a, 2002, 2009). Only four of the paleoclimatic perturbations are supported by appearance of poikilothermic–ectothermic large temnospondyls, because, like cuticular preservation required for studies of stomatal index (Retallack, 2002), large temnospondyls known from the Sydney Basin required exceptional preservation in black shales (Feistmantel, 1890; Woodward, 1890, 1908, 1931; Mitchell, 1924, 1925; Wade, 1935). Our study also includes locality details of U–Pb SHRIMP ages of zircons (Carr et al., 2003) used to reconcile advances in dating of Permian and Triassic rocks in Australia (Metcalfe et al., 2008) and in stratotype sections of China (Mundil et al., 2004; Lehrmann et al., 2006; Wignall et al., 2009).

2. Geological setting

The Sydney Basin, Permian–Triassic succession is largely outwash from the New England volcanic arc to the northeast, onlapping the older Lachlan Fold Belt to the southwest (Figs. 2 and 3; Mayne et al., 1974). This thick sequence includes numerous volcanic ashes, dated from zircons by $^{206}Pb/^{238}U$ geochronology using the SHRIMP instrument at the Australian National University Research School of Earth Sciences. Recent dates by Carr et al. (2003) (Table 1) using the SL13 standard are added to comparable published SHRIMP dates from the same laboratory (Gulson et al., 1990; Roberts et al., 1996) to develop a comprehensive local set of geochronological tie points (Fig. 4; Table 2). The SHRIMP age of Sri Lanka alluvial zircon standard SL13 was found by Black et al. (2003) to be 9% older than an IDTIMS age of the same standard (577.4 ± 1.2 versus 572 ± 0.4 Ma, respectively). This difference cannot be used for recalibration because of heterogeneity of the SL13 standard (Compston, 2001), as also indicated by broad errors (ca. ± 2 Ma 2σ). Nevertheless, our analyses are within error of recent redating of biostratigraphic boundaries of the Late Permian and Early Triassic (Mundil et al., 2004; Lehrmann et al., 2006; Ovtcharova et al., 2006), and about 2 Ma older than in the time scale of Gradstein et al. (2004).

Other constraints come from a few recognized paleomagnetic reversals found in volcanic lava flows (Fig. 4; Table 2). A complete magnetostratigraphy for the Sydney Basin is not available (Facer, 1981; Theveniaut et al., 1994), because of problems with Cretaceous paleomagnetic overprinting of sedimentary rocks (Foster and Archbold, 2001). The internationally correlated top of the long Kiaman paleomagnetic reversal is dated elsewhere at 265.5 Ma (Steiner, 2006), but has its type section in the top of the Dapto Latite flow 67 m below the Woonona Coal, near Kiama, in the coastal southern Sydney basin (Irving and Parry, 1963; Bowman, 1970; Facer, 1981). Unfortunately this level cannot be accurately correlated with the northern Hunter Valley (Figs. 1 and 3), because the Dapto Flow is part of an anomalously thick local stratovolcano (Raam, 1969; Retallack, 1999a), unrelated to local sequence stratigraphy (Arditto, 1991; Herbert, 1997a) or tephrostratigraphy (Kramer et al., 2001; Grevenitz et al., 2003).

The various radiometric and paleomagnetic tie points, which can be fixed to a specific meter level in a Camden–Murrays Run–Muswellbrook composite section (Fig. 4), either directly within the cores, or by sequence-stratigraphic correlation (Arditto, 1991; Herbert, 1997a,b) or tephrostratigraphy (Kramer et al., 2001; Grevenitz et al., 2003) are listed in Table 2. These are the basis for the age models shown in Fig. 5. The datum (0 m) for the composite section is the collar of Murrays Run bore hole, which has depths as positive numbers, so that section stratigraphically above that level has negative meter levels. The two Permian–Early Triassic age models (Muswellbrook and Murrays Run) are broadly similar, but Middle Triassic rocks (in Camden–Razorback sections) accumulated at a slower rate. The basal Hawkesbury Sandstone is a fluvial deposit with a source terrane in the southwest, where it eroded down into underlying units (Herbert, 1997b). Age models proposed here (Fig. 5) confirm that it is disconformable over the central Sydney Basin as well, at a time of reduced sedimentation rate.

Permian marine fossils of the Sydney Basin are endemic Gondwanan forms (Foster and Archbold, 2001), but a few cosmopolitan ammonoids and foraminifera allow correlation with international timescales. An Artinskian age was assumed by Glenister and Furnish (1961) for two species of ammonoids: "*Neocrimites*" *meridionalis* (Elderslie Formation, 30 m above Greta Coal Measures in the Maitland Colliery shaft near Farley), and "*Uraloceras*" *pokolbinensis* (Farley Formation, 3 miles southwest of Farley). Leonova and Bogolovskaya (1990) reassigned "*N.*" *meridionalis* to *Aricoceras*, a genus of late Artinskian to Wordian range (284.4–265.8 Ma in time scale of Gradstein et al., 2004). Schiappa et al. (2005) excluded "*Uraloceras*" *pokolbinensis* from the genus, and regard it as *Epijuresanites*, a genus of Kungurian (275.6–270.6 Ma) range (Popov, 2005; Leonova, 2007). In addition, the Mulbring Siltstone has yielded the Wordian (268.0–265.8 Ma) foraminiferan *Pseudonodosaria borealis* (Foster and Archbold, 2001).

Biostratigraphic control for the Triassic part of the section comes from Australian palynological zones (Foster and Archbold, 2001), which are now correlated internationally using conodonts in the Perth Basin, Western Australia. The upper *Protohaploxypinus microcorpus* palynozone, for example, has yielded the late Changsingian conodont *Neospathodus jolfensis*, and the lower *Lunatisporites pellucidus* palynozone has yielded the Dienerian–Smithian conodont *Neospathodus dieneri* (Metcalfe et al., 2008). Latest Permian and earliest Triassic rocks in the Sydney Basin are also confirmed by new radiometric

Fig. 2. Stratigraphic framework for major regions of the Sydney Basin showing (with gray highlight) coal seams correlated by sequence stratigraphy (Arditto, 1991; Diessel, 1992; Herbert, 1997a,b) and palynostratigraphy (McMinn, 1985), and tuffs correlated by tephrostratigraphy (Kramer et al., 2001; Grevenitz et al., 2003).

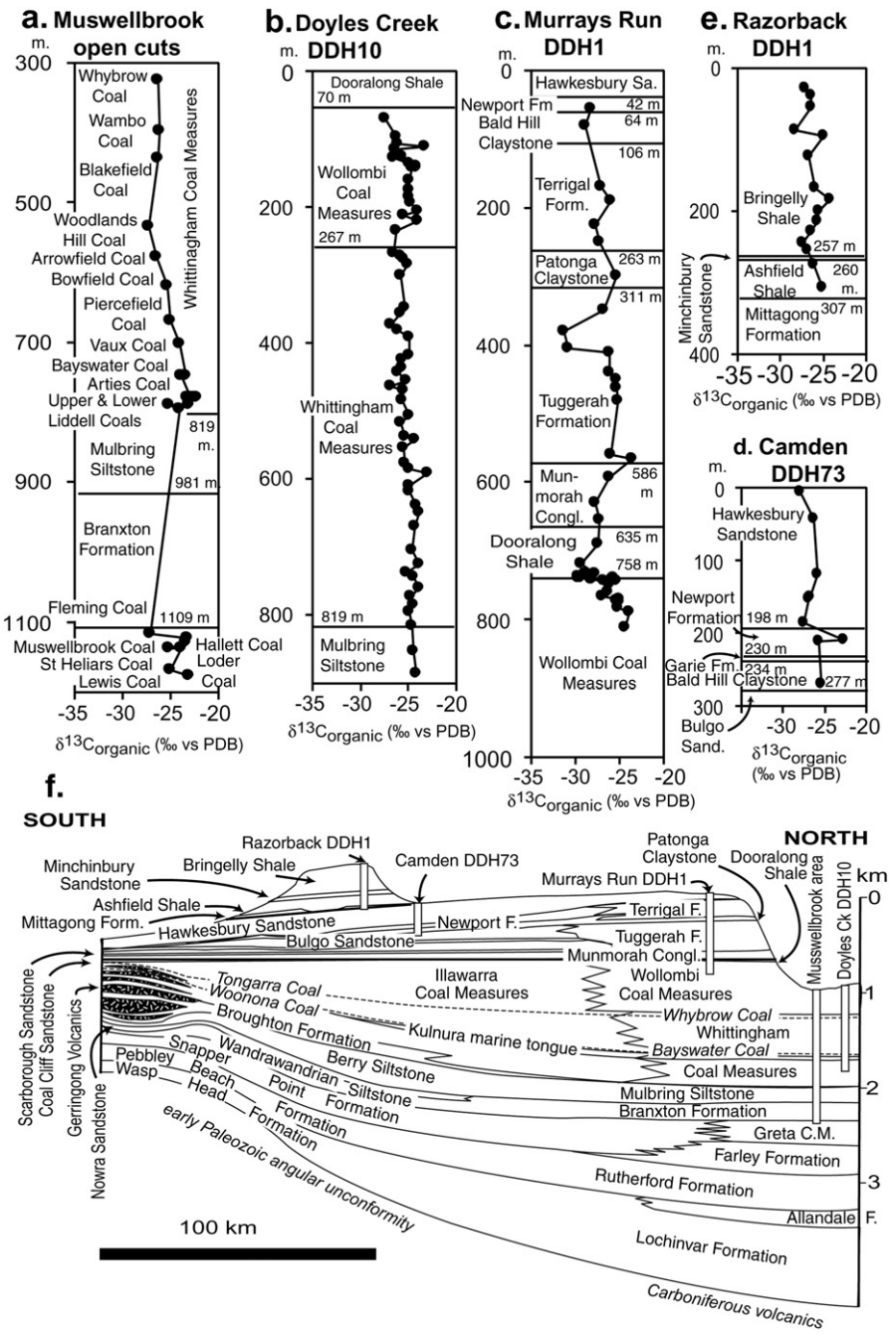

Fig. 3. Individual sections and cores analysed for organic carbon isotope composition (a–d) and their relative stratigraphic position in a north–south geological cross section (e) of the Sydney Basin along longitude 151°E (based on Raam, 1969; Mayne et al., 1974; Herbert, 1997a,b; Retallack, 1999a).

dating (Table 2). These new biostratigraphic and radiometric data settle concerns that the Permian–Triassic boundary in the Sydney Basin may have been disconformable (Retallack, 1980). There is onlap of several stratigraphic sequences in the southern coalfield near Wollongong, perhaps amounting to some 600,000 years, but this same sequence-stratigraphic study (Herbert, 1997b) detected no such break, but rather facies interdigitation in thick successions of backarc depocenters in the northern Sydney Basin.

3. Fossil evidence of CO_2 greenhouse crises

Several features of the Sydney Basin fossil plant and vertebrate record have been employed in this study to quantify atmospheric CO_2 and attendant changes in mean annual temperature and mean annual precipitation.

3.1. Lepidopteris stomatal index

Robust fossil cuticles of peltasperm seed fern leaves of the genus *Lepidopteris* provide proxies for atmospheric CO_2, because its stomatal apparatus is remarkably similar to that of living *Ginkgo*, whose stomatal index (percent stomates over epidermal cells) varies inversely with partial pressure of CO_2 (Retallack, 2009). In addition, the stomatal index of both *Ginkgo* and *Lepidopteris* associated within the same Triassic fossil deposit is very similar (Retallack, 2001a). *Ginkgo* leaves have low stomatal index (sparse stomates) when CO_2 is high and high stomatal index (dense stomates) when CO_2 is low to limiting, and this is not compromised by competing effects of aridity, salinity, and soil nutrient deficiency (Beerling and Royer, 2002). Another competing effect of volcanic SO_2 considered to compromise stomatal index as a proxy for CO_2 by Tanner et al. (2007) but disputed

Table 1
Details of recent SHRIMP U–Pb age determinations (Carr et al., 2003).

Location	Coordinates	Stratigraphic position	Age (Ma)	Sample	Comments
Freeway cut, Bulli Tops	S34.32926 E150.876231	Garie Formation	250.2 ± 2.5	PCF17	Age is from 17 analyses. An older group of 4 analyses gives 266.4 ± 4 Ma, and an older single grain gives ca. 355 Ma.
Nattai River	S34.43569 E150.45639	1 m above Farmborough Claystone	253.5 ± 2.4	PCF24	Age is from 15 of 18 analyses: 3 analyses gave ca. 266 Ma.
Joadga	S34.418983 E150.20718	Tuff just below Burragorang Claystone	255.9 ± 2.7	PCF22	The sample had two dominant modes and a single young analysis interpreted to have lost radiogenic Pb. The main age is from 9 analyses, but 5 analyses gives 266.1 ± 3.5 Ma.
Nattai River	S34.43569 E150.45639	Farmborough Claystone	256.5 ± 2.2	PCF23	Age is from 18 of 21 zircons analyzed: 2 are slightly older, 1 younger
Nattai River	S34.43569 E150.45639	Huntley Claystone	257.8 ± 2.3	PCW266	Age distribution is bimodal: 12 analyses at ca. 258 Ma, and 7 analyses at 266.6 ± 2.8 Ma. A younger grain may have lost Pb.
Nobbys Head	S32.919142 E151.79810	Awaba Tuff	259.7 ± 2.2	PCW325	This age is from 18 analyses. Two slightly younger ages are 245 Ma and 250 Ma, and one is older at ca. 272 Ma.
Mt Arthur	S32.329063 E150.86629	Fairford Formation	259.9 ± 2.8	PCF18	This age is from 20 of 23 areas analysed: 3 areas are interpreted to have lost radiogenic Pb.
Wollongong	S34.408237 E150.87857	2 m below top Broughton Formation	263.4 ± 2.4	PCF16	Age is from 19 analyses of 21 grains. Inherited zircons include ages of ca. 280, 300, 545 and 910 Ma. One grain has a 300 Ma rim and 545 Ma core

Note: $^{206}Pb/^{238}U$ SHRIMP dates using standard SL 13 made in Canberra by M. Fanning.

by Haworth et al. (2010), is unlikely in the Sydney Basin, where fossil leaves are hundreds of kilometers away from the active volcanic arc in highlands to the northeast (Fig. 1).

For this work, 44 cuticular preparations from 10 different stratigraphic levels were photographed and tallied for stomatal index (Fig. 4f; Table 3), supplementing other published stomatal index records from Australia, India and Russia (Retallack, 2002, 2009). All of these 10 collections meet the 500-cell rarefaction criterion of Retallack (2001a), but only half meet the 5-leaf-minimum rarefaction criterion of Royer et al. (2004). Only ten collections were available due to exceptional circumstances of rapid burial and prevention of decay required to preserve fossil plant cuticles (Jahren and Arens, 2009): most fossil plants in the Sydney Basin are preserved only as impressions (Retallack, 1980).

The paleobarometer devised by Retallack (2009) was used to estimate atmospheric CO_2 (C in ppmv) from stomatal index (I in %). This Eq. (1) was based on greenhouse experimental data with *Ginkgo* and on counting of herbarium specimens of *Ginkgo* collected during the rapid and ongoing post-industrial rise of atmospheric CO_2. The standard error of this relationship (±37 ppmv for Eq. (1)) is trivial compared with standard deviation of individual stomatal index measurements (averaging ± 0.16% and resulting in an average error +600/−446 ppmv for 10 pooled determinations). These standard deviations of the 10 pooled counts propagated through Eq. (1) are the errors presented in Table 2.

$$C = 294.1 + \left[\frac{1}{(4.84 \times 10^{-10})I^{7.93}}\right] \quad (1)$$

Atmospheric ppmv CO_2 estimated from stomatal index using Eq. (1) shows dramatic fluctuations (Table 3): upper Changsingian increase in the Sydney Basin to 7832 ppmv from Late Permian levels, which are estimated primarily from Russian leaves as 887 ppmv (Retallack, 2009). Other high values of CO_2 in the Sydney Basin include 2845 ppmv in the upper Changsingian, 3869 ppmv in the lower Griesbachian, 3510 ppmv in the lower Anisian, and 3756 ppmv in the basal Ladinian. These are extremely high CO_2 levels compared with preindustrial values of 280 ppmv (Alley et al., 2007), and include the highest known within the last 300 million years (Retallack, 2009).

These 10 stomatal index estimates of atmospheric CO_2 over 1 km of section and about 12 million years do not have the temporal resolution to detect paleoenvironmental volatility indicated by other proxies (Fig. 4), except for the interval of 17 m, representing perhaps 130,000 years, in the Garie and Newport Formations (Table 3). Over that interval, CO_2 declines from 3860 ppmv to near modern (305, then 417 ppmv), then abruptly rises to 3510 ppmv. Increase and draw-down of CO_2 from massive methane emissions on 100 kyr time scales have been modelled by Berner (2002). In his models, CO_2 levels above 1000 ppmv required degassing of the entire new volume of CH_4 or CO_2 in less than 3000 years, and draw-down to near-modern levels within a half million years required inputs over less than 30,000 years. Thus observed CO_2 fluctuation in the Newport Formation is feasible provided that atmospheric injections of CH_4 or CO_2 were individual events, massive in scale and very short in duration, such as the thermogenic liberation of CH_4 from intruded coal by individual flood basalt flows proposed by Retallack and Jahren (2008).

Minor local carbon-sinks for these abrupt CO_2 perturbations include carbonaceous shales of the lower Newport Formation (Retallack, 1975) and Gosford fish beds of the upper Newport Formation (Woodward, 1890). Other fish beds of comparable age (Spathian–Anisian) are known from non-marine carbonaceous shales of Tasmania (Dziewa, 1980), South Africa (McRae, 1999), Zambia (Jubb and Gardiner, 1975), Argentina (Hutchinson, 1973), France (Etter, 2002), and Germany (Schultze and Kriwet, 1999), and marine black shales of China (Tong et al., 2006), Greenland, Canada and Alaska (all three described by Schaeffer and Mangus, 1976). Short-term greenhouse crises and fish kills punctuated longer times of lower CO_2, and cooler and drier climates, as indicated by other proxies in the Sydney Basin (Fig. 4) and elsewhere (Retallack, 2005b, 2009).

Given the poor temporal resolution of the stomatal index record in the Sydney Basin (Fig. 4), it is remarkable that most of the Early Triassic paleoenvironmental deviations are represented by *Lepidopteris* leaves that are well preserved compared with other fossil plant localities near Sydney (Retallack, 1980). *Lepidopteris* leaves with low stomatal index (Fig. 6a–b) as a response to high CO_2, also had smaller stomates, thicker cuticles and much thicker leaves with less obvious venation than *Lepidopteris* with high stomatal index as a response to low CO_2 (Fig. 6c–d). By thickening cuticles and displacing oxygen from swampy sedimentary environments, greenhouse crises may have preferentially promoted preservation of leaves with high-CO_2 records (Retallack, 2009).

3.2. Lycopsid diversity

Early Triassic fossil floras of the Sydney Basin are marked by the extinction of *Glossopteris* and immigration of thermophilic plants whose Permian ancestral range was largely tropical (Retallack, 1997a,

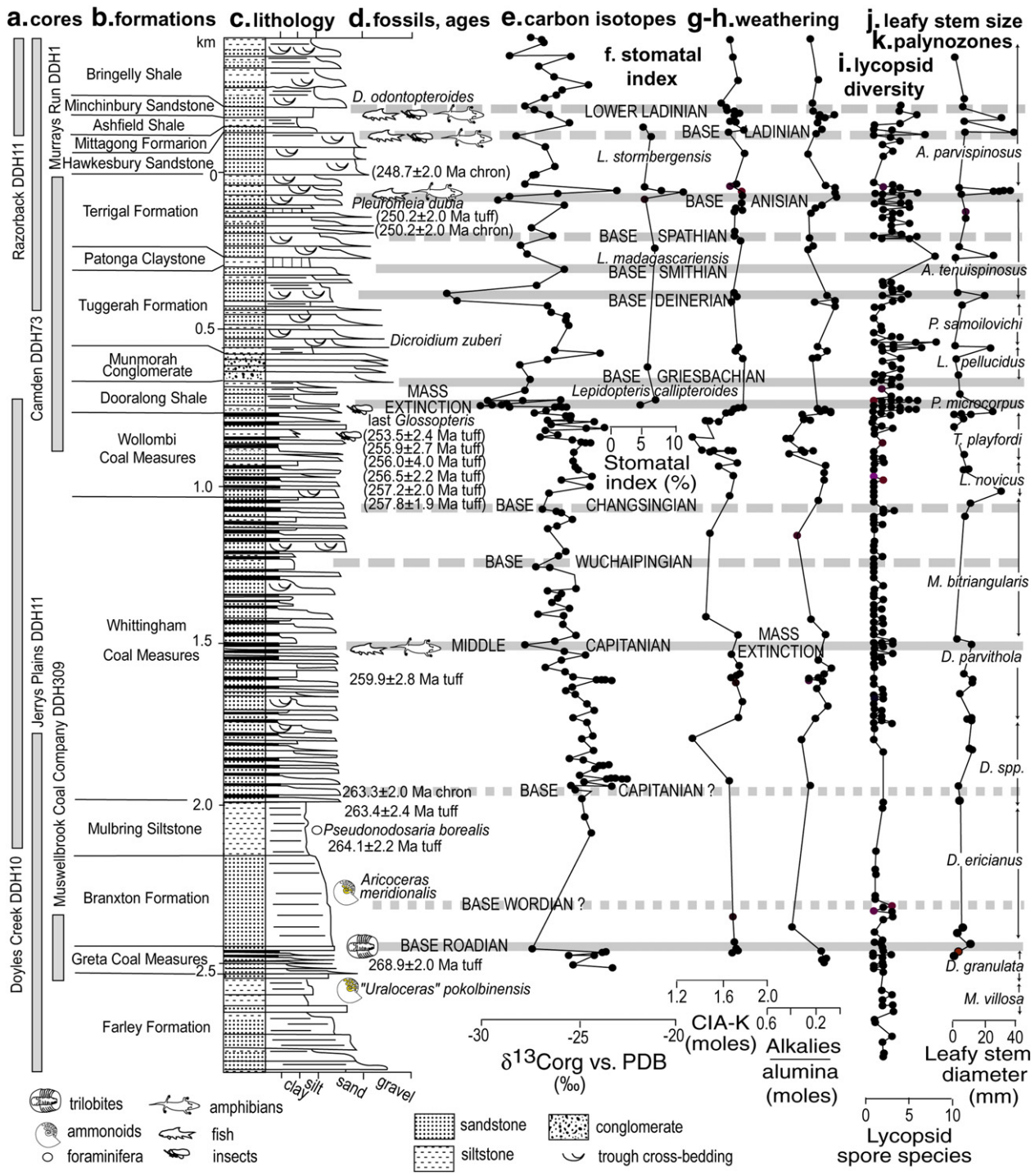

Fig. 4. Paleoenvironmental proxies for a Middle Permian to Middle Triassic composite section from boreholes in the northern and central Sydney Basin, Australia: a, boreholes used for section and carbon isotope analysis (see Fig. 1): b, geological formations: c, stratigraphic section: d, key fossils, paleomagnetic chrons, and radiometric ages: e, carbon isotopic values ($\delta^{13}C$ ‰) of bulk organic matter as a proxy for carbon cycle stability: f, stomatal index (%) of leaves of fossil *Lepidopteris* leaves as a proxy for atmospheric CO_2: g, chemical index of alteration without potash (molar ratio of alumina/alumina plus lime and soda) of paleosols (Bw and Bt horizons) as a proxy for mean annual precipitation: h, alumina/alkalies molar ratio of paleosols (Bw and Bt horizons) as a proxy for mean annual temperature: i, number of lycopsid spore species as a proxy for southerly migration of thermophilic plants: j, leafy stem diameter (mm) as a proxy for frost sensitivity: k, Sydney Basin palynozones of Helby (1973) and McMinn (1985).

2002), including wetland lycopsids such as *Tomiostrobus* and *Pleuromeia* (Fig. 7). Such tropical plants are remarkable for a region that during the Permian and Triassic was at a paleolatitude of 61°S (calculated from modern latitude of Sydney using Platetracker program of Scotese, 1997). Lycopsids are scarce during the Permian, and known only from a single occurrence of *Selaginella* (Townrow, 1968) and undescribed records of *Lycopodiopsis* (Rigby, 1964; Retallack, 1980). Triassic lycopsid megafossil occurrences are more widespread, but also patchy (Retallack, 1997a), and lycopsid diversity is much better represented by their spores. Sydney Basin lycopsid dispersed spores include the following genera: *Aratrisporites*, *Cirratriradites*, *Densoisporites*, *Endosporites*, *Gondisporites*, *Horstisporites*, *Laevigatosporites*, *Lundbladispora*, *Maiturisporites*, *Punctatisporites*, *Singhisporites*, *Tuberculatisporites*, and *Uvaesporites* (Balme, 1995). The stratigraphic distribution of these taxa within palynological preparations was compiled from publications (Grebe, 1970; Helby,

Table 2
Geochronological tie points for Murrays Run–Doyles Creek composite section.

Age (Ma)	CR (m)	MR (m)	M (m)	Nature	Location	Stratigraphic level (and correlatives)	Reference
248.7	520	42		Top Spathian paleomagnetic normal	Wollongong	Top Newport Formation	Facer, 1981; Ovtcharova et al., 2006; Steiner, 2006
250.2 ± 2.5	556	60		SHRIMP U/Pb zircon age	Bulli Heights	Lower Garie Formation tuff	Carr et al., 2003, herein
250.2	599	80		Base Spathian paleo-magnetic normal	Avon 52 core	20 m below top Bald Hill Claystone	Facer, 1981; Ovtcharova et al., 2006; Steiner, 2006
253.5 ± 2.4*		890	186	SHRIMP U/Pb zircon age	Nattai River	Farmborough Cl.(= Alcheringa C.)	Kramer et al., 2001; Carr et al., 2003, herein
255.9 ± 2.7		798	133	SHRIMP U/Pb zircon age	Joadja	Burragorang Clayst. (= Nalleen Tuff)	Kramer et al., 2001; Grevenitz et al., 2003; Carr et al., 2003, herein
256.0 ± 4.0		798	133	SHRIMP U/Pb zircon age	Awaba	Awaba Tuff (= Nalleen Tuff)	Gulson et al., 1990; Grevenitz et al., 2003
256.5 ± 2.2		890	186	SHRIMP U/Pb zircon age	Nattai River	Farmborough Cl.(= Alcheringa C.)	Kramer et al., 2001; Carr et al., 2003, herein
257.2		1040	267	Base Wuchiapingian paleomag. normal	Avon 5 core	2 m above Tongarra Coal (= base Wollombi CM)	Facer, 1981; Gradstein et al., 2004; Steiner, 2006
257.8 ± 2.3		1003	267	SHRIMP U/Pb zircon age	Nattai River	Huntley Claystone (= base Wollombi CM)	Herbert, 1997a; Carr et al., 2003
259.7 ± 2.2*		798	133	SHRIMP U/Pb zircon age	Nobbys Head	Awaba Tuff (= Nalleen Tuff)	Grevenitz et al., 2003; Carr et al., 2003, herein
259.9 ± 2.8		1784	660	SHRIMP U/Pb zircon age	Mt Arthur	Fairford Formation below Mt Arthur Coal	Carr et al., 2003, herein
263.3		1998	760	Base Capitanian paleomag. normal	Wollon-gong	30 m below top Pheasants Nest Formation (= Bulga Coal)	Irving and Parry, 1963; Bowman, 1970; Facer, 1981; Gradstein et al., 2004; Steiner, 2006
263.3		1998	800	Base Capitanian paleomag. normal	Muswellbrook	Lower Whittingham Coal Measures	Theveniaut et al., 1994; Foster and Archbold, 2001
263.4 ± 2.4		2000	819	SHRIMP U/Pb zircon age	Wollongong	Northfield Tuff (= upper Mulbring Siltstone)	Herbert, 1997a; Carr et al., 2003, herein
264.1 ± 2.2		2140	960	SHRIMP U/Pb zircon age	Muswellbrook	Lower Mulbring Siltstone	Roberts et al., 1996
268.9 ± 2		2461	1110	SHRIMP U/Pb zircon age	Muswellbrook	4 m above Fleming Coal, Greta Coal Measures	Roberts et al., 1996

Note: This table gives stratigraphic levels in Camden–Razorback core (CR), Murrays Run core (MR) and Muswellbrook core and outcrop (M) for new radiometric dates (Table 1) as well as for other published dates. Ages indicated by * were not used because contradicted by other ages for the same unit.

1973; McMinn, 1985; Glasspool, 2000a,b, 2003) and unpublished palynological reports by A. McMinn and R. Morgan of the Geological Survey of New South Wales (posted online at www.dpi.nsw.gov.au/minerals/geological/online-services/digs accessed March 1, 2009). A complete list of taxa and stratigraphic levels is available in Supplementary Data online.

These palynological data confirm that lycopsid spore diversity increased and fluctuated dramatically during the Early Triassic, but at only a few levels during the Permian (Fig. 4i). Stratigraphic intervals of diverse lycopsid spores are also narrow, as if incursions of thermophilic plants from the north were short lived.

3.3. Plant leafy stem size

Fossil palms, cacti, cycads and tree ferns are useful in paleoclimatology because their living relatives are intolerant of frost (Greenwood and Wing, 1995). Palms for example do not grow poleward of the −15 °C annual minimum isotherm, where their large terminal meristem is fatally frozen, even though they can recover from complete defoliation by freezing, and from loss to freezing of many roots (Sakai and Larcher, 1987). Permian and Triassic lycopsids (Fig. 7) are taxonomically unrelated to palms, but also had stout columnar trunks and a paleotropical distribution (Retallack, 1975, 1997a). In contrast, Permian glossopterids and cordaites of the Sydney Basin were trees similar to Triassic and living conifers in their short-shoot architecture (Retallack, 1980). In modern conifers also, frost tolerance is related to the size of shoot primordia and buds (Sakai and Larcher, 1987). An additional complication is that high atmospheric CO_2 (800 ppmv) has been shown in greenhouse experiments to raise the freezing temperature of plants, by 2.3–5.6 °C in the case of *Ginkgo biloba* (Royer et al., 2002). Because of this and tenuous relationships with modern plants, paleotemperature indications of likely frost-sensitive Permian and Triassic plants remain uncertain (Hermsen et al., 2009). Nevertheless, abrupt changes in fossil leafy stem (and inferred meristem) size may provide useful indications of paleoclimatic change. Fossil meristems are potentially preservable in permineralized Triassic and Permian plants (Hermsen et al., 2009), but the generally observed correlation between apical meristem diameter and leafy shoot diameter (Sakai and Larcher, 1987) has only been demonstrated quantitatively in cacti (Mauseth, 2004). Extension of this relationship to other plants, and to frost tolerance temperatures, could prove a promising avenue of future research.

The Sydney Basin has many horizons with measurable petiole widths and diameters of short shoots with attached leaves. Leafless long shoots or tree trunks with substantial woody thickening were ignored, because these plant parts show no known relationship with frost tolerance. Measurements were made on specimens in the Australian Museum and Geological Survey of New South Wales, and culled from publications (David, 1890; Feistmantel, 1890; Dun, 1898; Walkom, 1928, 1941; Townrow, 1968; Rigby, 1964, 1966, 1967, 1969; Retallack, 1975, 1980, 1997a; White, 1986; Diessel, 1992). Only the maximum value found at any one fossil locality is reported in Table 4. Raw measurements of petiole and leafy shoot diameters are plotted in Fig. 4j.

As would be expected for such high paleolatitudes, most Permian and many Triassic fossil leafy stems were slender (Table 4), like those of frost-tolerant temperate trees (Royer et al., 2002). Remarkably, the narrow stratigraphic intervals of large leafy stems and wide petioles, and inferred frost-sensitive terminal meristems, align with those of diverse lycopsid spores (Fig. 4). Stratigraphic intervals of these likely frost-sensitive plants are narrow, and may be evidence of brief incursions of tropical plants into temperate, high paleolatitude, vegetation of the Sydney Basin.

3.4. Ectotherm size

The frost line is a latitudinal barrier not only for palms and cycads (Greenwood and Wing, 1995), but also for crocodiles and alligators,

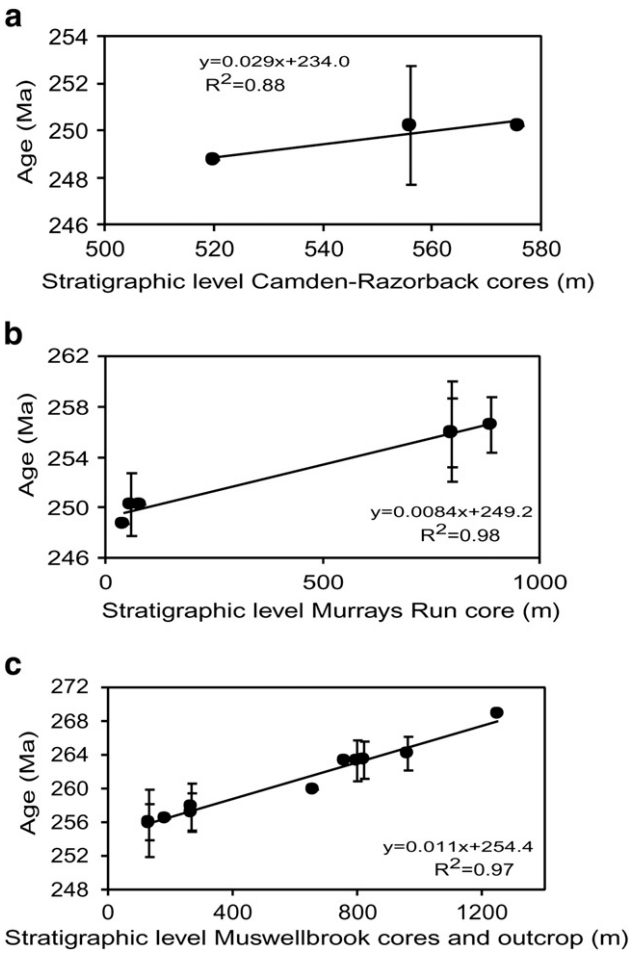

Fig. 5. Age models for Camden–Razorback (a), Murrays Run (b) and Muswellbrook–Doyles Creek (c) sections (see Table 2 for data points).

because of their ectothermic and poikilothermic physiognomy. The poleward spread of large ectotherms has thus been used a guide to global warming events of the past (Markwick, 1994). Similar arguments were used to infer frost-free climates during the Cretaceous from dinosaur fossils at high paleolatitudes in Victoria (Australia) and Alaska (USA), but dinosaurs are no longer regarded as fully ectothermic and also may have been capable of long migrations (Rich and Rich, 2000).

Temnospondyls were extinct aquatic ectotherms, very different from dinosaurs (Long, 1998), and are represented in Permian and Triassic rocks of the Sydney Basin by both footprints (Pepperell and Grigg, 1974; Naing, 1990) and skeletons (Welles and Cosgriff, 1965; Cosgriff, 1969, 1972, 1973). Only in a few cases, such as *Subcyclotosaurus davidi*, are complete skeletons known, but maximal sizes of temnospondyls can be estimated assuming body-part proportions comparable with *S. davidi* (Table 5). Unusually large ectotherms (>1 m length) for high paleolatitudes are found at three Triassic levels and one Middle Permian stratigraphic level, each with evidence from lycopsid spore diversity, and leafy stem diameter of frost-free paleoclimate. At other stratigraphic levels such fossils are small (Table 5). Large ectotherms may have been generally excluded from this region by low temperatures, and migrated south only during transient episodes of frost-free, greenhouse crises.

3.5. Vertebrate taphonomy

Vertebrate fossils are unknown in non-calcareous paleosols of the Sydney Basin (Retallack, 1997b, 2005b), in stark contrast with calcareous and little weathered paleosols of South Africa and Antarctica, often littered with bones of terrestrial tetrapods (Cosgriff et al., 1982; Retallack et al., 2003, 2006; Botha and Smith, 2006). Sydney Basin terrestrial tetrapods are represented by only a few trackways (Naing, 1990; Retallack, 1996). Articulated temnospondyl amphibians, fish, and insects are known from a handful of laminated black shale deposits (Tables 5 and 6), each only a few meters thick and now mostly exhausted by quarrying (Feistmantel, 1890; Woodward, 1890, 1908, 1931; Mitchell, 1924, 1925; Wade, 1935).

This feast and famine distribution of vertebrate fossils may have paleoclimatic implications. The general famine of vertebrates in paleosols of the Sydney Basin can be related to the propensity of bone to dissolve in acidic soils (Retallack, 1998), and acidic soils are in turn a consequence of humid climate and forest vegetation, as revealed by fossil plants, logs and soils (Retallack, 1999b). The local bounties of articulated fish fossils are at stratigraphic levels identified

Table 3
New estimates of stomatal index and atmospheric CO_2 from fossil *Lepidopteris* leaves.

Taxon	Locality	Coordinates	Formation	Level (m)	Age (Ma)	Specimens counted	C (#)	S (#)	L (#)	SI (%)	CO_2 (ppmv)
Lepidopteris stormbergensis	Woolloom-ooloo Bay	S33.869075 E151.216442	Basal Ashfield Shale	−162	242.87	MMF426	1209	67	1	5.35±0.16	3756+942/−721
Lepidopteris stormbergensis	Beacon Hill, Brookvale	S33.75379 E151.26285	Hawkesbury Sandstone	−132	244.56	AMF66281	623	38	3	6.06±0.27	1583+567/−379
Lepidopteris madagascariensis	Turimetta Head	S33.696308 E151.314077	Upper Newport Formation	45	249.58	AMF6398	1190	67	3	5.4±0.12	3510+605/−500
Lepidopteris madagascariensis	Birthday Shaft, Balmain	S33.852928 E151.175807	Middle Newport Formation	48	249.60	MMF12694	676	80	4	11.11±0.42	305+4/−3
Lepidopteris madagascariensis	Turimetta Head	S33.696308 E151.314077	Lower Newport Formation	55	249.66	AMF6400	6884	611	2	8.15±0.05	417±6
Lepidopteris madagascariensis	north of Mona Vale	S33.67522 E151.31971	Upper Garie Formation	62	249.72	AMF234205, AMF134199	1607	91	5	5.33±0.07	3860+364/−327
Lepidopteris madagascariensis	200 m south of Skillion	S33.450646 E151.449467	Terrigal Formation	251	251.31	AMF78033	2445	123	2	6.92±0.05	744+26/−25
Lepidopteris callipteroides	north of Coalcliff	S34.242294 E150.979598	Wombarra Shale	636	254.54	AMF51730, AMF51731	995	58	5	5.56±0.12	2845+476/−394
Lepidopteris callipteroides	north Coxs Gap tunnel	S32.435836 E150.207014	Dooralong Shale	747	255.47	MMF13719, MMF13721	8565	619	7	6.76±0.12	836+82/−70
Lepidopteris callipteroides	Oakdale Colliery	S34.043328 E150.483536	Basal Coalcliff Sandstone	758	255.57	AMF91443, AMF91444	3427	178	12	4.85±0.2	7832+2922/−2035

Notes: Specimens are from Australian Museum (AMF) and Geological Survey of New South Wales (MMF). Column head abbreviations are cells (C), stomata (S), leaves (L), and stomatal index (SI ± standard error of multiple counts). Stomatal index counts by C.A. Thompson and G.J. Retallack.

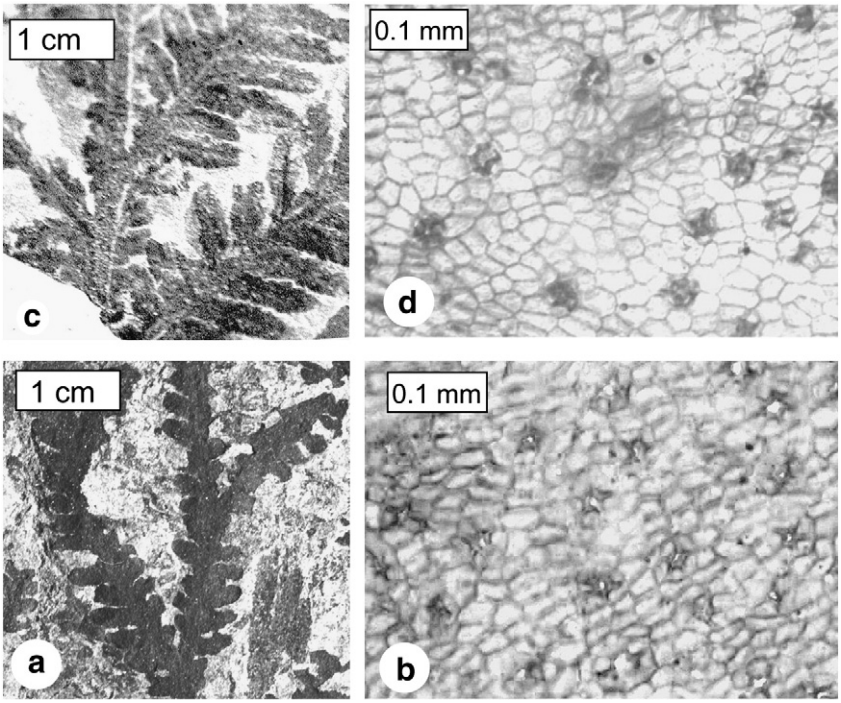

Fig. 6. *Lepidopteris callipteroides* (a–b) and *L. madagascariensis* (c–d) leaves (a, c) and cuticles (b, d) from Dooralong Shale at Coxs Gap (a, Australian Museum F91440, b NSW Geological Survey F13719a-5), and Newport Formation at Mona Vale (c, Australian Museum F78280) and Turimetta Head (d, Australian Museum F6400-6).

in previous paragraphs on stomatal index, lycopsid spore diversity, and leafy stem diameter as times of transient, unusually high CO_2, and frost-free, warm paleoclimate. Such transient events of the past are commonly associated with fine preservation of articulated fish and other fossils (Retallack, 2009). The modern CO_2 greenhouse crisis is a time of increasing storm intensity (Knutson et al., 2008) which does not entirely offset severe aquatic hypoxia (Hales et al., 2006). Such consequences of high CO_2 transients would have aided exceptional fossil preservation within narrow zones of organic shales, as found in the Sydney Basin (Fig. 4; Tables 5 and 6).

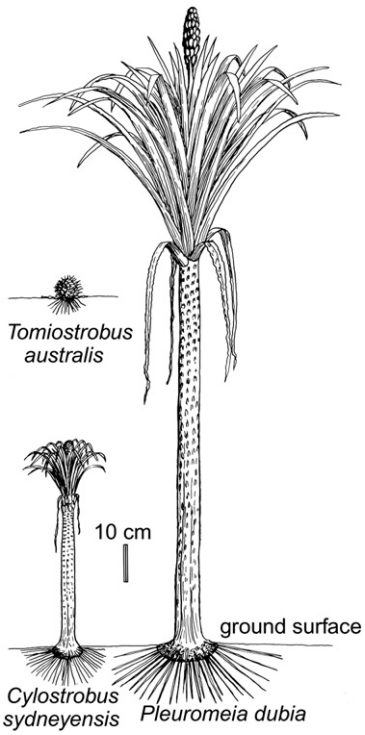

Fig. 7. Reconstructions of Early Triassic lycopsid megafossil species found in the Newport Formation from Long Reef north to Avalon, New South Wales (after Retallack, 1997a).

4. Paleosol indicators of greenhouse crises

Other sources of paleoclimatic information are paleosols within wetland and alluvial sedimentary rocks of the Sydney Basin (Fig. 8). Some Early Triassic paleosols were Ultisols (Retallack, 1997b), not known currently to extend further south or north than 47° latitude because they require at least 11 °C mean annual temperature and 1186 mm mean annual precipitation (Retallack, 2008). In contrast are periglacial paleosols (Retallack, 1999a), marine dropstones (Fielding et al., 2008) and ikaite pseudomorphs (Selleck et al., 2007; Frank et al., 2008; Birgenheier et al., 2010) of the early Late Permian of the Sydney Basin, compatible with a paleolatitude of 61°S (Scotese, 1997). Such divergent indications of paleoclimate also have come from local kaolinitic clays, comparable with those created by tropical weathering, within a sequence that includes glacial deposits (Loughnan, 1991).

4.1. Paleosol paleoclimatic methods

This study offers quantitative estimates of mean annual precipitation and temperature and of long term weathering from chemical composition of paleosol clayey (Bt) and weathered (Bw) horizons, compiled from prior studies (Retallack, 1997b, 1999b) and newly analysed (using XRF by ALS Chemex of Vancouver British Columbia, Canada and in the Department of Earth Sciences, Royal Holloway, University of London; see Supplementary Data online for raw analyses and their stratigraphic levels).

Sheldon et al. (2002) have devised a paleohyetometer for mean annual precipitation (P in mm) from modern soils from chemical index of alteration (A in mol%mol^{-1}): a molar ratio of alumina over alumina plus lime and soda multiplied by 100 (Sheldon et al., 2002). The ratio is based on the standard equation of hydrolytic weathering

Table 4
Leafy shoot diameters and lycopsid megafossil diversity.

Plant locality	Coordinates	Formation	Taxon of terminal meristem	Terminal meristem diam. (μm)	Leafy shoot (mm)	Lycopsid species	Level (m)	Age (Ma)	Reference
Clarkes Hill, near Cobbitty	S33/998050 E150.689458	Bringelly Shale	*Rissikia* "*media*"	325	2	0	−361	232.8	Retallack, 1980
Glenlee	S34.087264 E150.756454	Bringelly Shale	*Dicroidium zuberi*	356	8	0	−241	236.3	Retallack, 1980
Cranebrook	S33.9718547 E150.729527	Minchinbury Sandstone	*Dicroidium odontopteroides*	351	7	0	−221	236.9	Retallack, 1980
Erskineville	S33.901703 E151.190737	Ashfield Shale	*Isoetes* sp.	488	33	1	−180	238.1	Australian Museum AMF16178
St Peters	S33.909515 E151.184155	Ashfield Shale	*Ginkgoites simmondsii*	362	9	0	−170	238.4	Retallack, 1980
Woolloom-ooloo	S33.869075 E151.216442	Mittagong Formation	*Dicroidium zuberi*	356	8	0	−164	238.6	Retallack, 1980
Cockatoo Dock	S33.846337 E151.172406	Hawkesbury Sandstone	cf. *Williamsonia*	536	42	0	−135	239.4	Geological Survey MMF3080
Beacon Hill	S33.75379 E151.26285	Hawkesbury Sandstone	*Dicroidium zuberi*	356	8	0	−134	239.4	Retallack, 1980
north of Avalon Beach	S33.625819 E151.340492	Newport Formation	*Taeniopteris lentriculiforme*	335	4	0	43	249.6	Retallack, 1980
north of Avalon Beach	S33.633872 E151.337568	Newport Formation	*Cladophlebis oblonga*	504	36	0	48	249.6	Retallack, 1980
south of Whale Beach	S33.614335 E151.332543	Newport Formation	*Pleuromeia dubia*	467	29	1	50	249.6	Retallack, 1980, 1997a
Long Reef to Avalon	S33.696308 E151.314077	Newport Formation	*Cylostrobus sydneyensis*	446	25	3	51	249.6	Retallack, 1980, 1997a
Mona Vale	S33.67522 E151.31971	Newport Formation	*Pleuromeia dubia*	483	32	1	53	249.6	Retallack, 1975, 1980, 1997a
north of Bungan Beach	S33.664712 E151.322866	Newport Formation	*Dicroidium zuberi*	346	6	0	54	249.7	Retallack, 1975, 1980, 1997a
Garie Beach	S34.167767 E151.075100	Newport Formation	*Dicroidium narrabeenensis*	356	8	0	120	250.2	Retallack, 1980
Mt Piddington	S33.606047 E150.253283	Wentworth Falls Clay.	*Dicroidium zuberi*	356	8	0	135	250.3	Retallack, 1980
Birthday Shaft	S33.852928 E151.175807	Newport Formation	*Lepidopteris madagascariensis*	335	4	0	231	251.1	Retallack, 1980
Skillion, Terrigal	S33.450646 E151.449467	Terrigal Formation	*Tomiostrobus australis*	451	26	1	251	251.3	Retallack, 1980
Birthday Shaft	S33.852928 E151.175807	Bulgo Sandstone	"*Sagenopteris*" *salisburoides*	325	2	0	262	251.4	Retallack, 1980
Birthday Shaft	S33.852928 E151.175807	Bulgo Sandstone	"*Zeugophyllites*"	330	3	0	375	252.4	Retallack, 1980
Moore Park	S33.889774 E151.219003	Bulgo Sandstone	Rhizophore	425	21	1	390	252.5	Retallack, 1980
Birthday Shaft	S33.852928 E151.175807	Bulgo Sandstone	*Sphenopteris* sp.	351	7	0	420	252.7	Retallack, 1980
92mELECOM Wyong DDH4	S33.175122 E151.381528	Tuggerah Formation	*Brachyphyllum* sp.	325	2	0	550	253.8	Australian Museum AMF51456
Cudgegong Rd, Kandos	S32.86830 E149.975257	Dooralong Shale	*Isoetes* sp.	446	25	2	560	253.9	Retallack, 1980, 1997a
Coxs Gap	S32.435836 E150.207014	Dooralong Shale	*Lepidopteris callipteroides*	341	5	0	595	254.2	Retallack, 1980, 2002
Birthday Shaft	S33.852928 E151.175807	Wombarra Shale	*Lepidopteris callipteroides*	341	5	0	650	254.7	Retallack, 1980, 2002
Coalcliff	S34.242294 E150.979598	Coal Cliff Sandstone	*Lepidopteris callipteroides*	341	5	0	698	255.1	Retallack, 1980, 2002
Bulli	S34.332433 E150.908912	Coal Cliff Sandstone	*Isoetes beestoni*	446	25	2	757	255.6	Retallack, 1980, 1997a
Victoria Pass, Mt Victoria	S33.581690 E150.237047	Katoomba Coal	*Selaginella harrisiana*	320	1	0	759	255.6	Townrow, 1968
Mt Keira, Wollongong	S34.404432 E150.850984	Bulli Coal underclay	*Gangamopteris walkomii*	341	5	0	760	255.6	Rigby, 1964; White, 1986
Duncans Pass	S33.811671 E150.265442	Katoomba Coal	*Glossopteris linearis*	378	12	0	761	255.6	Rigby, 1967

Maloneys Quarry	S33.491335 E149.78881	Illawarra Coal Measures	*Glossopteris* "*linearis*"	351	7	0	763	255.6	White, 1986
Talbragar River	S32.073988 E149.738249	Illawarra Coal Measures	*Blechnoxylon talbragarense*	325	2	0	764	255.6	White, 1986
Mt Keira, Wollongong	S34.404690 E150.851032	Balgownie Coal	*Glossopteris browniana*	367	10	0	768	255.7	Rigby, 1964; White, 1986
Flagstaff Hill, near Newcastle	S32.925314 E151.791137	Newcastle Coal Meas.	*Sphenopteris lobifolia*	351	7	0	776	255.7	White, 1986
Fennell Bay	S32.994454 E151.601135	Awaba Tuff base	*Selaginella* sp.	320	1	0	798	255.9	Diessel, 1992, p.29
Belmont	S32.986496 E151.664859	Cruadace Bay Form.	*Glossopteris indica*	335	4	0	818	256.1	Walkom, 1928
Mt Keira, Wollongong	S34.405522 E150.851594	Wongawilli Coal	*Sphenopteris lobifolia*	351	7	0	886	256.6	Rigby, 1964; White, 1986
Apple Tree Creek, near Jerrys Plains	S32.497734 E150.861489	Middle Wollombi Coal Meas.	*Neomariopteris* sp.	351	7	0	900	256.8	Retallack, 1980
Mt Keira, Wollongong	S34.405522 E150.851594	Below Wongawilli Coal	*Glossopteris browniana*	367	10	0	941	257.1	Rigby, 1964; White, 1986
Mt Keira, Wollongong	S34.407240 E150.853598	Lower American Creek C.	*Sphenopteris lobifolia*	351	7	0	942	257.1	Rigby, 1964; White, 1986
Little Redhead, NE of Dudly	S32.969173 E151.736356	Above Victoria Tunnel C.	*Glossopteris ampla*	378	12	0	960	257.3	Retallack locality L285
Merewether Beach South	S32.933626 E151.782795	Above Yard Coal	*Cordaicladus adamsi*	488	13	0	1005	257.6	Rigby, 1969
Bakers quarry, 1 km east of Morpeth	S32.741798 E151.627751	Upper Tomago Coal Meas.	*Gangamopteris obovata*	378	12	0	1040	257.9	Retallack personal observations 1967
18 km south of Singleton	S32.725275 E151.177118	Upper Malabar Formation	*Glossopteris decipiens*	362	9	0	1100	258.4	Retallack locality L45
Ulan	S32.247467 E149.758171	Ulan Coal	*Walkomiella australis*	330	3	0	1485	261.7	White, 1986
Ulan	S32.247467 E149.758171	Ulan Coal,	*Squamella* sp.	384	13	0	1489	261.7	White, 1986
Bowenfels, east of Lithgow	S33.471087 E150.139760	Irondale Coal	*Gangamopteris clarkeana*	362	9	0	1596	262.6	Feistmantel, 1890
Blackmans Flat (Swamp) north of Lithgow	S33.360963 E150.061760	Above Lidsdale Coal	*Glossopteris taeniopteroides*	378	12	0	1608	262.7	Feistmantel, 1890
Mt Kembla, Wollongong	S34.461814 E150.803939	Woonona Coal-2.5 m	*Gangamopteris obovata*	378	12	1	1618	262.8	Rigby, 1964; White, 1986
Waniora Point	S34.339260 E150.925990	Lower Erins Vale Form.	Gymnospermae gen. indet.	341	5	0	1650	263.1	Retallack personal observations 2007
Wongawilli	S34.476307 E150.750612	1 m below Figtree Coal	*Glossopteris ampla*	378	12	0	1733	263.8	Rigby, 1964; White, 1986
Wongawilli	S34.476307 E150.750612	2 m below Figtree Coal	*Glossopteris* sp	362	9	0	1734	263.8	Rigby, 1964; White, 1986
Wongawilli	S34.476307 E150.750612	3 m below Figtree Coal	*Glossopteris ampla*	378	12	0	1735	263.8	Rigby, 1964; White, 1986
Wongawilli	S34.478286 E150.755184	Unanderra Coal + 2 m	*Glossopteris browniana*	367	10	0	1826	264.5	Rigby, 1964; White, 1986
Wongawilli	S34.478286 E150.755184	Unanderra Coal + 1 m	*Glossopteris communis*	372	11	0	1827	264.5	Rigby, 1964; White, 1986
Wongawilli	S34.478286 E150.755184	Unanderra Coal top	*Gangamopteris obovata*	378	12	0	1828	264.6	Rigby, 1964; White, 1986
Wongawilli	S34.478286 E150.755184	Unanderra Coal-4 m	*Cyclodendron leslii*	378	12	1	1834	264.6	Rigby, 1964
Rix's Creek	S32.533088 E151.25035	Above Liddell Coal	*Glossopteris clarkei*	341	5	0	1945	265.5	Feistmantel, 1890
Bellambi Pool	S34.35516 E150.92473	Pheasants Nest Form.	Gymnospermae gen. indet.	341	5	0	1988	265.9	Retallack personal observations 2007
Wongawilli	S34.480388 E150.752541	Berkeley Sill top	*Glossopteris cordata*	341	5	0	1998	266.0	Rigby, 1964; White, 1986
Anvil Creek, Branxton	S32.652975 E151.357372	Uppermost Greta CM	*Stellotheca robusta*	356	8	0	2400	269.4	Rigby, 1966
Muswellbrook Open Cut Mine	S32.237826 E150.940220	Upper Greta CM	*Stellotheca* sp.	335	4	0	2412	269.5	Rigby, 1966
Richmond Vale colliery	S32.855462 E151.476726	Upper Greta CM	*Glossopteris sp.*	378	12	0	2450	269.8	David, 1890; White, 1986
Stony Creek, near Branxton	S32.664552 E151.324797	Lower Greta CM	*Glossopteris browniana*	341	5	0	2480	270.0	Feistmantel, 1890
Burning Mountain	S31.856311 E150.98033	Lower Greta CM	*Umbellaphyllites ivini*	322	1.5	0	2495	270.2	Walkom, 1941

Table 5
Measured and estimated (from skull length) lengths of temnospondyls.

Species	Locality	Coordinates	Formation	Level (m)	Age (Ma)	Skull length (mm)	Body length (mm)	Skull-predicted length (m)	References
Notobrachyops picketti	Mortdale	S33.976434 E151.081513	Ashfield Shale	−180	238.1	33	Partial	0.1353	Cosgriff, 1973
Limnopus sp	Macquarie Fields	S33.993697 E150.878152	Ashfield Shale	−170	238.4	575	2041	2.0505	Pepperell and Grigg, 1974
Subcylcotosaurus davidi	St Peters	S33.909515 E151.184155	lower Ashfield Shale	−165	238.5	584	2072	2.0823	Welles and Cosgriff, 1965
Parotosaurus brookvalensis	Beacon Hill	S33.75379 E151.26285	Hawkesbury Sandstone	−132	239.5	66	Partial	0.2519	Welles and Cosgriff, 1965
Blinasaurus wilkinsoni	Gosford	S33.423571 S151.339185	upper Terrigal Formation	44	249.6	25	Partial	0.107	Cosgriff, 1969
Parotosaurus wadei	Gosford	S33.423571 S151.339185	upper Terrigal Formation	44	249.6	66	200	0.2519	Cosgriff, 1972
Limnopus sp	Turimetta Head	S33.696308 E151.314077	lower Newport Formation	60	249.7	391	Partial	1.4003	Naing, 1990
Bothriceps australis	Airly	S33.111417 E150.014367	Lithgow Coal	1873	264.9	81	Partial	0.3049	Cosgriff, 1969, 1973
Trucheosaurus major	Airly	S33.111417 E150.014367	Lithgow Coal	1873	264.9	152	618	0.5558	Cosgriff, 1969, 1973

in which lime and soda are depleted as alumina is enriched during weathering (Retallack, 2001b). Sheldon et al. (2002) give this relationship ($R^2 = 0.72$, S.E. = ± 181 mm) as the following Eq. (2).

$$P = 221.1e^{0.0197A} \quad (2)$$

This proxy relationship yields paleoprecipitation estimates that are consistent with independent proxies such as plant fossil-based estimates (Hamer et al., 2007a,b).

A paleosol paleothermometer of Sheldon et al. (2002) estimates mean annual temperature (T in °C) from the molar ratio of alkalies (potash plus soda) over alumina (R in mol mol^{-1}) of paleosol subsurface clayey (Bt) horizons. This alkali ratio is inversely proportional to mean annual temperature in modern soils, presumably because of the more effective desalinization of soils in less evaporative cool climates. As devised by Sheldon et al. (2002), this relationship ($R^2 = 0.37$, S.E. = ± 4.4 °C) is Eq. (3) as follows.

$$T = -18.52R + 17.22 \quad (3)$$

This proxy relationship yields paleotemperature estimates that are consistent with independent proxies such as plant fossil-based estimates (Hamer et al., 2007a,b).

Another useful proxy devised by Sheldon and Tabor (2009) gives long-term changes in weathering (ΔW in mol mol^{-1} from the following Eq. (4)) from deviation of chemical index of alteration for a particular paleosol (A_x in mol mol^{-1} derived from molar abundances of major element oxides such as Ca_m from the following Eq. (5)) from a mean value for the entire sequence (μ in mol mol^{-1}). This proxy for changes in degree of weathering is especially useful for long successions of paleosols developed on sedimentary parent materials, as is the case for the Sydney Basin, because it filters out an averaged component of weathering from source terrains. Eq. (4) from Sheldon and Tabor (2009) gives this relationship, whose error envelope (Fig. 9) is determined by the analytical error of analyses (2σ analytical uncertainties are 0.83 wt.% for Al_2O_3, 0.22 wt.% for CaO, 0.11 wt.% for Na_2O, and 0.13 wt.% for K_2O).

$$\Delta W = A_x - \mu \quad (4)$$

$$A_x = 100 \cdot \frac{Al_m}{Al_m + Ca_m + K_m + Na_m} \quad (5)$$

These various proxies are based largely on modern North American soils, which are partly volcaniclastic, middle to high latitude soils of recently glaciated terrains (Sheldon et al., 2002), and comparable in these respects with Permian and Triassic paleosols of the Sydney Basin (Retallack, 1997b, 1999b). In such a setting, redeposited alumina is a local confounding factor for paleoclimatic estimates, recognized by kaolinitic breccias (Loughnan, 1991; Retallack, 2005a), rather than a pervasive bias, as it is in Australia's current highly aluminous subtropical soils (Retallack, 2008). Another problem for some of these paleoclimate estimates may be potassium enrichment during illitization of smectite (Retallack, 1997b, 1999b) under burial conditions creating bituminous coal in both Permian and Middle Triassic parts of the succession (Diessel, 1992). This had limits because maximum potash content observed was 5.66 wt.%. Increased potash during burial would lower absolute temperature estimates and increase weathering estimates, but preserve relative paleoclimatic spikes of most interest for this study.

Table 6
Lengths of largest complete fossil fish.

Largest species	Locality	Coordinates	Formation	Level (m)	Age (Ma)	Length (mm)	Reference
Palaeoniscus antipodeus	Gibraltar Tunnel	S34.458019 E150.420063	Upper Wiananatta Shale	−200	237.5	187	Feistmantel, 1890
Myriolepis pectinatus	St Peters	S33.909515 E151.184155	Lower Ashfield Shale	−170	238.4	376	Woodward, 1908
Myriolepis clarkei	Cockatoo Dock	S33.846337 E151.172406	Hawkesbury Sandstone	−132	239.5	526	Feistmantel, 1890
Macroaethes brookvalensis	Beacon Hill	S33.75379 E151.26285	Hawkesbury Sandstone	−132	239.5	299	Wade, 1935
Myriolepis clarkei	Gosford	S33.423571 S151.339185	Upper Gosford Formation	44	249.6	434	Woodward, 1890
Urosthenes latus	Merewether Beach	S32.933626 E151.782795	Above Yard Coal	1005	257.6	350	Feistmantel, 1890
Elonichthys davidi	Hexham	S32.829256 E151.683128	61 m below Borehole Coal	1121	258.6	252	Mitchell, 1924, 1925
Urosthenes latus	Lithgow	S33.477786 E150.175737	Lithgow Coal	1873	264.8	320	Woodward, 1931

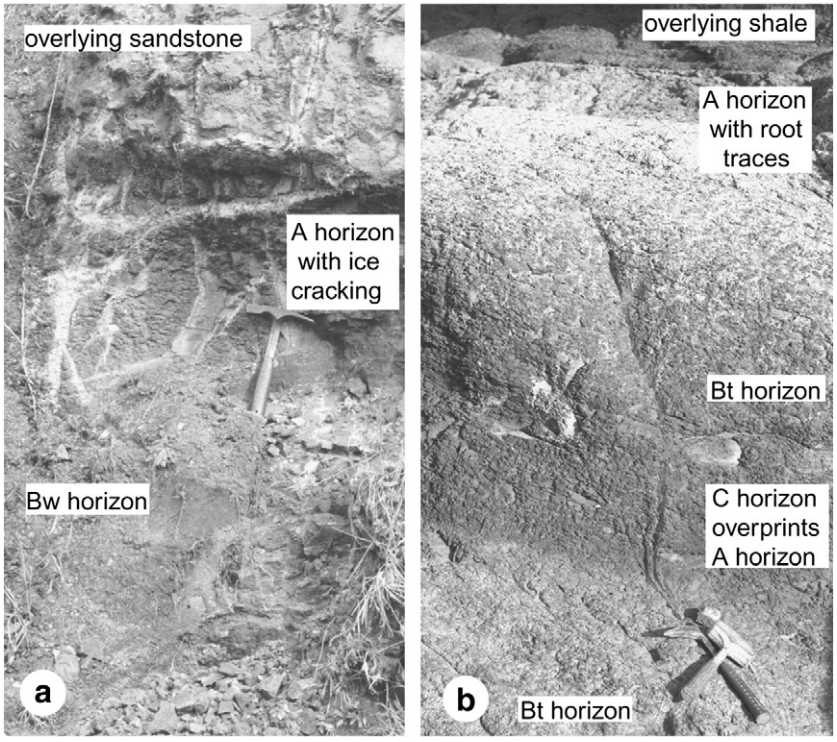

Fig. 8. (a) Loveleigh clay paleosol (Haploturbel) near Kiama, compared with (b) Long Reef clay paleosol (Hapludult) near Long Reef: (a) is a periglacial palaeosol with ice deformation (Retallack, 1999a), whereas (b) is a deeply weathered temperate forest paleosol with abundant drab-haloed root traces (Retallack, 1997b).

4.2. Paleosol paleoclimatic record

Application of these climofunctions to paleosols in the Sydney Basin show nine transient increases in mean annual precipitation and temperature (Fig. 9f–g). Paleotemperatures, estimated in this way, were largely cool temperate (~8 °C) with transient excursions to warm temperate (~13 °C) in the Köppen climate classification (Trewartha, 1982). Seasonally deciduous leaves and strong growth

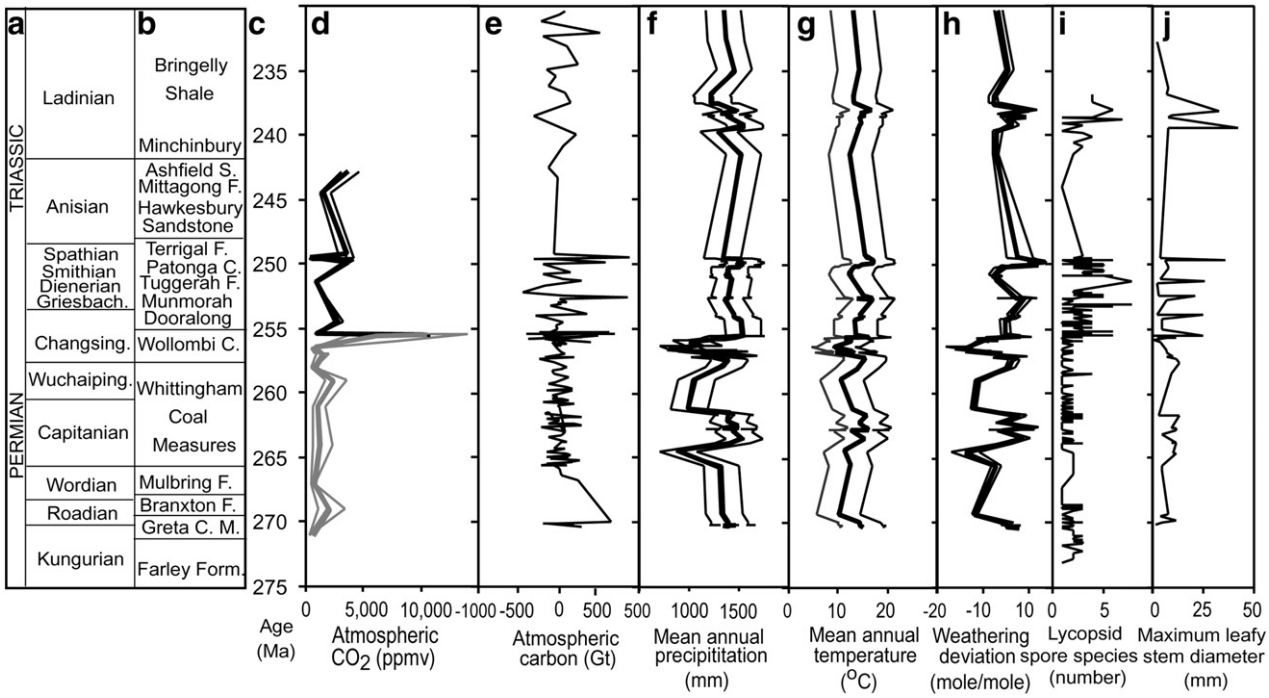

Fig. 9. Time series of paleoenvironmental change from the Middle Permian to Middle Triassic in the Sydney Basin, Australia: a, time scale for Triassic and Permian (after Gradstein et al., 2004; Henderson, 2005; Lehrmann et al., 2006; Ovtcharova et al., 2006): b, stratigraphic units of northern Sydney Basin (Figs. 2–4): c, age (Ma) using local age models (Fig. 5a–b): d, atmospheric CO_2 (ppmv) estimated from stomatal index of leaves of *Lepidopteris* from the Sydney Basin (black: latest Permian and Triassic only: Table 3), and of *Lepidopteris* and *Tatarina* from Russia and India (gray: Permian from Retallack, 2009): e, release to the atmosphere (+ve) and non-atmospheric sequestration (−ve) of carbon (Gt) calculated from carbon isotope values compared with Late Permian (Wuchaipingian and Changhsingian) atmospheric carbon: f, mean annual precipitation (mm) computed from paleosol (Bw and Bt horizon) CIA-K; g, mean annual temperature (°C) computed from paleosol (Bw and Bt horizon) alkalies/alumina: h, deviation of chemical weathering compared with average for section (mole/mole): i, diversity of thermophilic plants from lycopsid spore species: j, maximum leafy shoot diameter (mm), as a guide to frost sensitivity of plants.

rings in fossil wood, are supporting indications of a cold, probably snowy, season (Retallack and Jahren, 2008). Ice deformation structures in paleosols (Gelisols) are evidence that some parts of the late Middle and early Late Permian were frigid (Retallack, 1999a). Ikaite pseudomorphs (also called glendonites after Glendon Brook in the Hunter Valley) are supporting evidence of cold Permian marine waters during deposition of the Branxton, Farley and correlative formations (Selleck et al., 2007; Frank et al., 2008; Fielding et al., 2008; Birgenheier et al., 2010). Such frigid conditions are not apparent from Late Permian or Triassic paleosols in the Sydney Basin.

Paleoprecipitation estimates from geochemical climofunctions were more or less humid in both Permian and Triassic, generally 1000–1200 mm with fluctuations up to ~1600 mm mean annual precipitation (Fig. 9f). This amount of precipitation in a temperate climate with low evapotranspiration during the growing season is compatible with the absence of calcareous paleosols (Aridisols) and abundance of coals (Histosols) among paleosols of the Sydney Basin, unlike Histosol-poor and Aridisol-rich aridland Middle Permian–Triassic sequences such as the Karoo Basin, South Africa (Retallack et al., 2003). Coals are limited to the Permian part of the Sydney Basin sequence, because their host plants were extinguished during the Late Permian (Retallack et al., 1996), but humid climate persisted to create kaolinitic and hematitic well drained paleosols (Ultisols, Spodosols and Alfisols) during the Early Triassic. Comparable modern soilscapes, climate and deciduous vegetation are found today in southern Canada, northeastern United States, and northern Europe (Retallack, 1999b).

Increases in chemical index of alteration (Fig. 9g) are promoted by both higher temperature and precipitation, and emphasize the spiky nature of the Sydney Basin paleoclimate record (Fig. 9). The increase in chemical weathering during Late Permian mass extinction (Fig. 7g) is consistent with previous records of enhanced short-term chemical weathering during this crisis from Antarctica (Sheldon, 2006), South Africa (Retallack et al., 2003), New Mexico (Retallack, 2009), and Texas (Retallack, 2005b), which suggests that this is a global rather than local signal. Increased weathering corresponds with increases in CO_2, and increased diversity and diameter of lycopsids (Fig. 9i–j), so exactly as to support the concept that these events were greenhouse crises. They are crises because many of these events are major mass extinctions, particularly the Late Permian (Jin et al., 2001) and Middle Permian (Wignall et al., 2009) mass extinctions. Spathian and Smithian events of the Early Triassic were also profound biotic turnovers (Payne et al., 2004). They are greenhouse events because warm-wet climatic transients at high latitudes coincided with episodes of high atmospheric CO_2 (Fig. 9d) as in other comparable paleoclimatic records (Retallack, 2009).

5. $\delta^{13}C$ quantification of greenhouse crises

Carbon isotope analyses of kerogen, fossil plant debris, and coal reflect dramatic variation in the isotopic composition of the atmosphere sampled by plants (Arens et al., 2000). Remarkable volatility in atmospheric carbon isotopic composition is known to be global in distribution across the Permian–Triassic boundary (de Wit et al., 2002; Retallack et al., 2006). Negative excursions of −6‰ $^{13}C_{org}$ cannot be explained by any reasonable scenario of productivity or biomass lost to mass extinction, or of carbon release by volcanic degassing or bolide vaporization (Retallack and Krull, 2006). Such negative spikes in atmospheric carbon isotopic composition can only come from injections into the atmosphere of large amounts of isotopically light carbon from marine methane clathrates or from thermal metamorphism of coal (Berner, 2002, 2006; Retallack and Jahren, 2008).

Chemical analysis of cuticles has proven best for inferences concerning atmospheric isotopic composition (Jahren and Arens, 2009), but cuticles are not common in the Sydney Basin (Retallack, 1980). In Late Permian Coals of Wybung Head, near Newcastle, Retallack and Jahren (2008) analysed bulk coal and cuticle separates, finding no difference in organic carbon isotope composition. For this study, bulk composition of carbonaceous shales was analysed, with care to sample away from known paleosols, because paleosol organic matter is known to be up to 2‰ $\delta^{13}C$ heavier in water-stressed soils (Bestland and Krull, 1999), and in biologically active well drained soils (Wynn, 2007). Siderite in some Sydney Basin paleosols (Retallack, 1997b, 1999a) was also avoided, because it yielded anomalously high values and carbonate of waterlogged paleosols cannot be considered a proxy for atmospheric composition (Tabor et al., 2007). Carbon isotopic data of Morante (1996) for shales of the Murrays Run core were augmented by numerous new analyses of fresh carbonaceous rock from other Sydney Basin drillcores (Fig. 4e), analysed on an Isochron EA continuous flow to a VG Isotech Optima Mass Spectrometer in Royal Holloway University of London. See Supplementary Data online for raw analyses and their stratigraphic levels.

5.1. Atmospheric perturbation

Profound perturbations of the carbon isotopic composition of atmospheric CO_2 require injections of carbon with different isotopic composition, and the amounts of such injections can be calculated following the mass balance formulation of Jahren et al. (2001). The mass of carbon (N in Gt = Pg = 10^{15} g) of a given carbon isotope composition ($\delta^{13}C_e$) required for such atmospheric isotopic transients results in a later isotopic composition ($\delta^{13}C_a$) that balances the previous mass of atmospheric carbon (M in Gt) and its isotopic composition ($\delta^{13}C_b$) according to Eq. (6).

$$(M+N)\left(\delta^{13}C_a\right) = M\left(\delta^{13}C_b + N\delta^{13}C_e\right) \quad (6)$$

This relationship has been used (by Retallack and Jahren, 2008) to calculate transient emission to the atmosphere of at least 640 Gt during the Late Permian mass extinction and 221 Gt C during the Middle Permian mass extinction, assuming thermogenic methane ($\delta^{13}C$ of −55‰) emission into Late Permian 1385 ppmv CO_2, and middle Permian 947 ppm CO_2 (Retallack, 2009), and Late Permian organic matter at $\delta^{13}C$ of −25.47‰ (average of Late Permian values). Here a revised Late Permian value of 887 ppmv CO_2 (from Retallack, 2009) has been used to estimate both emissions (positive values) and sequestrations (negative values) from one carbon isotopic determination to the next as a minimal guide to gigatonnes (Gt) of carbon moving into and out of the atmosphere from the Middle Permian to the Middle Triassic (Fig. 9e).

These minimal estimates of carbon mass distributions across the Permian–Triassic boundary support two conclusions: (1) the carbon amounts are very large, comparable with the current mass of all atmospheric carbon (600 Gt; Sigman and Boyle, 2000; Berner, 2002; Retallack and Jahren, 2008), and (2) Early Triassic and late Middle Permian volatility contrast with Late Permian and Middle Triassic stability (Payne et al., 2004).

There also is evidence of Late Permian sulfur cycle crises (Riccardi et al., 2007; Meyer et al., 2008), not addressed by this study of carbon cycle crises. The carbon and sulfur crises could be related because hydrogen sulfide would be released to the atmosphere from water bodies stagnating in a CO_2 greenhouse crisis. Alternatively, sulfur pollution of the atmosphere could have come independently from volcanic gases or bolide impact-vaporization of evaporites (Riccardi et al., 2007). Dramatic changes in atmospheric sulfur loads would also have had marked paleoclimatic effects.

5.2. Isotopic chemostratigraphy

Changes in atmospheric carbon isotopic composition are global, because the atmosphere is well mixed on time scales of 2–10 years (Revelle and Suess, 1957; Levin et al., 1992), and international

correlation of carbon isotope fluctuations is not surprising (Retallack et al., 2006). Biostratigraphic correlations from ammonoids, foraminifera, and pollen give only general alignment of correlative sections (Fig. 4), but as for magnetostratigraphy (Steiner, 2006), isotopic proxies for atmospheric composition can be aligned on specific isochronous isotopic inflections. Such correlations of marine and non-marine sequences gain strength from multiple excursions. Graphic correlation as envisaged by Shaw (1964) is used here to correlate different marine and non-marine isotopic records to our record for the Sydney basin. Graphic correlation of isotopic inflections between the Murrays Run sections and sections elsewhere in the world (Fig. 10j) are all highly significant ($R^2 = 0.99$). These high correlations are evidence that events unequally spaced in time are reflected in events proportionally represented through stratigraphic sections. The slopes of the lines are different, because of different sediment accumulation rates in each section. Some slopes are negative and some positive because some sections are boreholes with stratigraphic level measured down-hole, and others are sections with stratigraphic level measured up-section.

Graphic correlation of carbon isotopic spikes also allows international correlation of our new organic $\delta^{13}C$ records (Fig. 9a–c) with marine Chinese sections (Fig. 9f–i). Marine biostratigraphy of Chinese limestones (Payne et al., 2004; Wignall et al., 2009), reveals that the basal Smithian and Spathian are marked by positive carbon isotope anomalies, and basal Anisian is between a marked negative and positive anomaly (Payne et al., 2004), but other biostratigraphic boundaries are negative carbon anomalies of varying magnitude, with the late Changsingian and basal Wuchaipingian especially marked (Riccardi et al., 2007; Wignall et al., 2009). Unfortunately, several marine carbon isotope records from China are not long enough to reveal multiple excursions needed for accurate graphic correlation, but the Late Permian to Early Triassic lower Guandao section does show multiple excursions and tight correlation with the Murrays Run section (Fig. 9j). Tightening of these correlations not only improves land–sea event reconstruction, but offers new geochronological tie points for poorly fossiliferous, non-marine sequences.

6. Discussion

Refined age and proxy paleoenvironmental data presented here have implications for both the precise geological dating of the two great Permian mass extinctions and for the hypothesis of prolonged versus delayed recovery from mass extinction.

6.1. Mass extinction ages revised

The Permian–Triassic boundary in the stratotype section near Meishan, China, is defined by the first appearance of a newly evolved Triassic conodont, *Hindeodus parvus*, which is 17 cm above the marine mass extinction level, the facies change, and the negative carbon isotope anomaly (Jin et al., 2001). In thicker Western Australian marine sections the first Triassic conodonts are 10 m above the mass extinction of the *Glossopteris* palynoflora and the carbon isotope anomaly, and the basal Triassic is marked by the *Kraeuselisporites septatus* palynozone (Metcalfe et al., 2008), which is equivalent to the *Lunatisporites pellucidus* palynozone in the Sydney Basin (Foster and Archbold, 2001). Within the tectonically active northern Sydney Basin (Moonshine 13 and Murrays Run cores), the glossopterid mass extinction, carbon isotope shift and last coal are separated by the *Protohaploxypinus microcorpus* palynozone, some 40 m thick, below the base of the *Lunatisporites pellucidus* palynozone within the Munmorah Conglomerate and Dooralong Shale (Morante, 1996). In

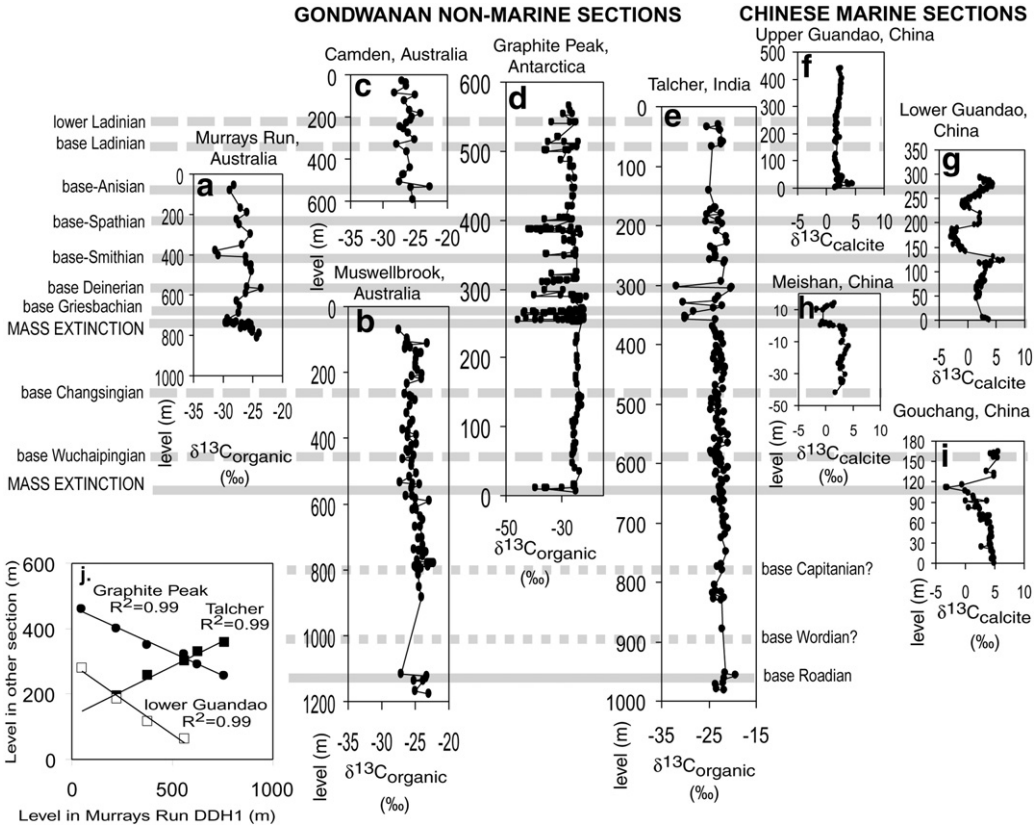

Fig. 10. Organic carbon isotope chemostratigraphy of selected sequences. Carbon cycle perturbations in these non-marine Gondwanan and marine Chinese sections have spacing that is statistically indistinguishable ($R^2 = 0.99$ in h), despite greatly varied local sedimentation rates. Isotopic data for the Sydney Basin is largely new, but includes data from Compston (1960), Philip and Saxby (1979), and Morante (1996). Isotopic and biostratigraphic data from other sections is from Krull and Retallack (2000), Wit et al. (2002), Payne et al. (2004), Retallack et al. (2006), Riccardi et al. (2007), and Wignall et al. (2009).

China, Western Australia and Sydney Basin, the mass extinction and associated carbon isotope anomaly is not at the very end of the Permian. Our age model for Murrays Run (Fig. 5b) yields 253.9 ± 2.7 Ma for the Permian–Triassic boundary and 255.6 ± 2.7 for the mass extinction and carbon isotope anomaly. These are indistinguishable (within error) from more precise dating of a Chinese section at Shangsi suggesting that the Permian–Triassic boundary defined at the first appearance of the conodont *Hindeodus parvus* was about 251.9 ± 0.3 Ma, and that the earlier mass extinction and carbon isotope anomaly was at 252.6 ± 0.2 Ma (Mundil et al., 2004).

Similarly, re-examination of the mass extinction during the Middle Permian in China now finds that mass-extinction and a large carbon-isotope negative excursion is within the *Jinogondolella altudaensis* conodont zone of the mid-Capitanian (Wignall et al., 2009) at about 263 Ma in the time scale of Henderson (2005). There is an additional carbon-isotope negative excursion at the top of the Capitanian (Wang et al., 2004) defined by the first appearance of the conodont *Clarkina postbitteri* subspecies *postbitteri* in a cline from subspecies *C. p. hongshuiensis* and placed at about 260.4 Ma (by Henderson, 2005). This later event is not such a profound faunal overturn as the mass extinction now dated as mid-Capitanian (rather than end-Capitanian or end-Guadalupian), which has been correlated with mass extinction of glossopterid plants and dinocephalian tetrapods coincident with a marked carbon isotope negative excursion on land in South Africa and Antarctica (Retallack et al., 2006). Lucas (2009) follows Losovsky (1998) in placing a comparable extinction of tetrapods in paleomagnetically constrained sections in Russia below the end of the Kiaman reversal (265.5 Ma; Steiner, 2006), well before the end of the Capitanian and Guadalupian (260.4 Ma; Henderson, 2005). Golubev (2005) in contrast uses similar paleomagnetic and faunal data to place the Russian tetrapod extinction at the end-Guadalupian, and also reveals that temporal spacing of the Russian tetrapod localities cannot resolve the issue there. Two negative carbon isotope anomalies in the Sydney Basin section (Fig. 4e) are now dated by our Murrays Run age model (Fig. 5b): one at 259.8 ± 2.7 Ma within the Wambo Coal (seam 36 of Konecki, 1953; Compston, 1960), and another more marked anomaly at 261.8 ± 2.7 Ma in the Woodlands Hill Coal (seam 26 of Konecki, 1953; Compston, 1960). The Wambo Coal anomaly may be equivalent to the basal Wuchaipingian negative excursion of Wang et al. (2004) and the Woodlands Hill Coal anomaly equivalent to mid-Capitanian mass extinction and isotopic anomalies recognized in China (Wignall et al., 2009), Antarctica and South Africa (Retallack et al., 2006). Another negative excursion in the Fleming Coal of the Greta Coal Measures (Fig. 2) is dated by our Murrays Run age model (Fig. 5b) at 270.0 ± 2.7 Ma, straddling the Kungurian–Wordian boundary (Gradstein et al., 2004). Potential basal Capitanian and basal Wordian isotopic markers are inadequately sampled in our time series, but these levels are indicated by Wordian marine fossils, *Aricoceras* and *Pseudonodosaria* in the northern Sydney Basin (Leonova and Bogolskaya, 1990; Foster and Archbold, 2001).

These new discoveries call for reconsideration of the terms "end-Guadalupian" (Clapham et al., 2009) and "end-Permian" (Song et al., 2009) for the big Late Paleozoic mass extinctions. They are really Middle Permian (or middle Capitanian) mass extinctions, and Late Permian (or late Changsingian) mass extinctions, respectively. The terms Permian–Triassic and Middle–Late Permian extinctions are still appropriate, because the aftermath of both mass extinctions lasted through the formal boundaries. These changes in terminology are the result of increased temporal resolution between extinction horizons defined on last appearances and biostratigraphic boundaries defined on first appearances of newly evolved taxa (Jin et al., 2001; Henderson, 2005).

6.2. Long recovery or repeated blows?

Our newly age-calibrated multiproxy records from the Sydney Basin do not favor the hypothesis that prolonged recovery of biota from Late Permian extinction was due to the severity of extinctions, but rather the alternative hypothesis of repeated environmental trauma of multiple postapocalyptic greenhouse episodes. Extraordinary atmospheric injections of isotopically light carbon, perhaps from thermal metamorphism of coal by feeder dikes to Siberian Trap lavas (Retallack and Jahren, 2008), may have created successive CO_2 greenhouse crises that repeatedly spread thermophilic plants and deep weathering southward to near the Antarctic Circle. A comparable mass balance argument has been made that the Middle Permian carbon isotope anomaly and mass extinction was produced by intrusion of coals by the Emeishan Trap lavas of China (Retallack and Jahren, 2008). Whether such mass balance arguments link other isotopic anomalies to coal intrusion remains to be seen: asteroid impact, methane clathrate destabilization, and biomass destructions remain plausible cause of lesser carbon isotope anomalies and CO_2 greenhouse crises (Retallack and Krull, 2006). There were at least 5 of these transient greenhouse crises within the 4 million years after the Late Permian mass extinction (Jin et al., 2001; Retallack et al., 2003, 2006), including Smithian and Spathian crises (Payne et al., 2004), and other biotic overturns (Ovtcharova et al., 2006).

Each greenhouse crisis provided short episodes with a similar set of selection pressures of varied intensity that drove some organisms to extinction and others to migration. Generally cool, subhumid, low CO_2 conditions were punctuated by brief episodes of warm, humid high CO_2 conditions (Fig. 10). For marine and lacustrine invertebrates, surges of hypercapnia (high CO_2) selected for small organisms with high surface-area to volume ratio and active respiratory ventilation, such as clams and ammonoids. Episodes of lowered oceanic pH and oxygenation were especially hard on invertebrates with passive respiration, such as corals and bryozoans (Knoll et al., 2007). For terrestrial vertebrates, pulses of lowered oxygenation of air may have provided respiratory challenges akin to those faced by mountaineers today at high altitudes (Retallack et al., 2003; Huey and Ward, 2005). For wetland plants such as *Glossopteris*, already on the edge of adequate oxygen for root respiration in their peaty substrates, episodes of lowered oxygenation became lethal hypoxia (Sheldon and Retallack, 2002). Herbaceous lycopsids such as *Tomiostrobus* (Fig. 5) with their hollow rootlets and shallow corms would have fared better in hypoxic wetland soils and lakes (Retallack, 1997a). Thus the distinctive biota of the Early Triassic may not have been merely a legacy of the greatest known mass extinction, but maintained by multiple postapocalyptic greenhouse crises.

7. Conclusions

Our multiproxy study of Permian and Triassic non-marine strata of the Sydney Basin of southeastern Australia has confirmed organic carbon isotope anomalies coincident with Late Permian and Middle Permian mass extinctions (Retallack et al., 2006). Refined stratigraphic analysis demonstrates that mass extinctions were not at the very end of the Late or Middle Permian (contrary to Clapham et al., 2009; Song et al., 2009), but before upper boundaries of the Late Permian (Changsingian) and Middle Permian (Capitanian) in China (Jin et al., 2000; Metcalfe et al., 2008; Wignall et al., 2009). In addition to these marked perturbations of the carbon cycle additional negative carbon isotope anomalies were found during the Early Triassic, in contrast with an isotopically quiet Late Permian and Middle Triassic, as previously noted in marine records (Payne et al., 2004). Our studies of stomatal index of fossil plants from the Sydney Basin demonstrate that this Early Triassic episode of carbon isotopic volatility was also a time of fluctuating levels of atmospheric CO_2. Additional evidence from the chemical composition of paleosols reveals that these CO_2 crises were also times of elevated temperatures and precipitation, which also were opportunities for transient migrations of lycopsids and large amphibians south into this high latitude region. The biota of the Early Triassic was not merely an aftermath of an unusually

profound mass extinctions, but maintained by successive greenhouse crises.

Acknowledgments

Steven Hall and Michael Silbern helped with core sampling from the NSW Mineral Resources Core Library. Robert Jones, Ian Percival, and John Pickett facilitated loans of fossil cuticles from the Australian Museum and NSW Geological Survey. Nathalie Grassineau (Royal Holloway University of London) helped obtain new carbon isotope analyses. Paul Wignall and Jonathan Payne graciously supplied marine isotopic data. Diligent reviewing above and beyond the call of duty by Thomas Algeo and Carl Brett greatly improved this manuscript.

Appendix A. Supplementary data

Supplementary data to this article can be found online at doi:10.1016/j.palaeo.2010.09.022.

References

Alley, R., Berntsen, T., Bindoff, N.I., et al., 2007. Climate Change 2007: The Physical Science Basis. Intergovernmental Panel on Climate Change, Geneva.
Arditto, P.A., 1991. A sequence stratigraphic analysis of the Late Permian succession in the Southern Coalfield, Sydney basin, New South Wales. Aust. J. Earth Sci. 38, 125–137.
Arens, N.C., Jahren, A.H., Amundson, R., 2000. Can C_3 plants faithfully record the carbon isotopic composition of atmospheric carbon dioxide? Paleobiology 26, 137–164.
Balme, B.E., 1995. Fossil *in situ* spores and pollen grains; an annotated catalogue. Rev. Palaeobot. Palynol. 87, 81–322.
Beerling, D.J., Royer, D.L., 2002. Reading a CO_2 signal from fossil stomata. New Phytol. 153, 387–397.
Berner, R.A., 2002. Examination of hypotheses for the Permo-Triassic boundary extinction by carbon cycle modelling. U.S.A. Nat. Acad. Sci. Proc. 99, 4172–4177.
Berner, R.A., 2006. The carbon and sulfur cycles and atmospheric oxygen from Middle Permian to Middle Triassic. Geochim. Cosmochim. Acta 69, 3211–3217.
Benton, M.J., Tverdokhlebov, V.P., Surkov, M.V., 2004. Ecosystem remodelling among vertebrates at the Permian–Triassic boundary in Russia. Nature 432, 97–100.
Bestland, E.A., Krull, E.S., 1999. Palaeoenvironments of early Miocene Kisingiri volcano *Proconsul* sites: evidence from carbon isotopes, palaeosols and hydromagmatic deposits. J. Geol. Soc. Lond. 156, 965–976.
Birgenheier, L.P., Frank, T.D., Fielding, C.R., Rygel, M.C., 2010. High latitude, Permian bulk organic carbon isotopic curve reveals CO_2 variations coupled with multi-million year glacial and non-glacial climatic fluctuations, eastern Australia. Palaeogeogr. Palaeoclimatol. Palaeoecol. 286, 178–193.
Black, L.P., Kamo, S.L., Williams, I.S., Mundil, R., Davis, D.W., Korsch, R.J., Foudoulis, C., 2003. The application of SHRIMP to Phanerozoic geochronology; a critical appraisal of four zircon standards. Chem. Geol. 200, 171–188.
Blakey, R.C., 2008. Gondwana paleogeography from assembly to breakup a 500 m.y. odyssey. In: Fielding, C.R., Frank, T.D., Isbell, J.L. (Eds.), Resolving the Late Paleozoic Ice Age in time and space: Geol. Soc. Amer. Spec. Pap., 441, pp. 1–28.
Botha, J., Smith, R.M.H., 2006. Rapid vertebrate recuperation in the Karoo Basin of South Africa following the end-Permian extinction. J. Afr. Earth Sci. 45, 502–514.
Bowman, H.N., 1970. Paleonvironment and revised nomenclature of the upper Shoalhaven Group and Illawarra Coal Measures in the Wollongong–Kiama area, New South Wales. Geol. Surv. NSW Rec. 12, 163–182.
Calder, J.H., Gibling, M.R., Scott, A.C., Davies, S.J., Hebert, B.L., 2006. A fossil lycopsid forest succession in the classic Joggins section of Nova Scotia: paleoecology of a disturbance-prone Pennsylvanian wetland. In: Greb, S.F., DiMichele, W.A. (Eds.), Wetlands through Time: Geol. Soc. Amer. Spec. Pap., 399, pp. 169–195.
Carr, P.F., Fanning, M., Jones, B.G., Hutton, A.C., 2003. Geochronology of coal measures in the Sydney Basin from U–Pb SHRIMP dating of airfall tuffs. In: Hutton, A.C., Jones, B.G., Carr, P.F., Ackerman, B., Switzer, A.D. (Eds.), 35th Sydney Basin Symp. Univ. Wollongong Proc., pp. 303–305.
Clapham, M.E., Shen, S.-Z., Bottjer, D.J., 2009. The double mass extinction revisited: reassessing the severity, selectivity and causes of the end-Guadalupian biotic crisis (Late Permian). Paleobiology 31, 32–50.
Compston, W., 1960. The carbon isotope composition of certain marine invertebrates and coals from the Australian Permian. Geochim. Cosmochim. Acta 18, 1–22.
Compston, W., 2001. Effect of Pb loss on the ages of reference zircons QGNG and SL13, and of volcanic zircons from the Early Devonian Merrions and Turondale Formations, New South Wales. Aust. J. Earth Sci. 48, 797–803.
Cosgriff, J.W., 1969. *Blinasaurus*, a brachyopid genus from Western Australia and New South Wales. R. Soc. NSW J. 52, 65–88.
Cosgriff, J.W., 1972. *Parotosaurus wadei*, a new capitosaurid from New South Wales. J. Paleontol. 46, 545–555.
Cosgriff, J.W., 1973. *Notobrachyops picketti*, a brachyopid from the Ashfield Shale, Wianamatta Group, New South Wales. J. Paleontol. 47, 1094–1101.
Cosgriff, J.W., Hammer, W.R., Ryan, W.J., 1982. The Pangaean reptile, *Lystrosaurus maccaigi*, in the Lower Triassic of Antarctica. J. Paleontol. 56, 371–385.
David, T.W.E., 1890. Note on the occurrence of *Glossopteris* in a remarkable state of preservation in the Greta Coal—measures at Richmond Vale near Maitland. Linn. Soc. NSW Proc. 5, 424–426.
de Wit, M.J., Ghosh, J.G., de Villiers, S., Rakotosolofo, N., Alexander, J., Tripathi, A., Looy, C., 2002. Multiple organic carbon isotope reversals across the Permo-Triassic boundary of terrestrial Gondwana sequences; clues to extinction patterns and delayed ecosystem recovery. J. Geol. 110, 227–246.
Diessel, C.F.K., 1992. Coal-Bearing Depositional Systems. Springer, Berlin.
Dun, W.S., 1898. Additions to the Permo-Carboniferous flora of New South Wales, 2. Geol. Surv. NSW Rec. 6 (1), 46–51.
Dziewa, T.J., 1980. Early Triassic osteichthyans from the Knocklofty Formation of Tasmania. Pap. Proc. R. Soc. Tas. 114, 145–160.
Etter, W., 2002. *Grés à Voltzia*: preservation in early Mesozoic deltaic and marginal marine environments. In: Bottjer, D.J., Etter, W., Hagadorn, J.W., Tang, C.M. (Eds.), Exceptional Fossil Preservation: A Unique View of the Evolution of Marine Life. Columbia University Press, New York, pp. 205–220.
Facer, R.A., 1981. Palaeomagnetic data for Permian and Triassic rocks from drill holes in the southern Sydney Basin, New South Wales. Tectonophysics 74, 305–321.
Feistmantel, O., 1890. Geological and palaeontological relations of the coal and plant-bearing beds of Palaeozoic and Mesozoic age in eastern Australia and Tasmania. Geol. Surv. NSW Palaeontol. Mem. 3, 1–183.
Fielding, C.R., Frank, T.D., Birgenheier, L.P., Rygel, M.C., Jones, A.T., Roberts, J., 2008. Stratigraphic record and facies associations of the late paleozoic ice age in eastern Australia (New South Wales and Queensland). In: Fielding, C.R., Frank, T.D., Isbell, J.L. (Eds.), Resolving the Late Paleozoic Ice Age in Time and Space: Geol. Soc. Amer. Spec. Pap., 441, pp. 41–57.
Foster, C.B., Archbold, N.W., 2001. Chronologic anchor points for the Permian and Early Triassic of the Eastern Australian basins. In: Weiss, R.H. (Ed.), Contributions to the Geology and Paleontology of Gondwana in Honour of Helmut Wopfner. Geological Institute, University of Cologne, pp. 175–197.
Fraiser, M.L., Bottjer, D.J., 2004. The non-actualistic Early Triassic gastropod fauna: a case study of the Lower Triassic Sinbad Limestone Member. Palaios 19, 259–275.
Fraiser, M.L., Bottjer, D.J., 2007. Elevated atmospheric CO_2 and the delayed biotic recovery from the end-Permian mass extinction. Palaeogeogr. Palaeoclimatol. Palaeoecol. 252, 164–175.
Frank, T.D., Thomas, S., Fielding, C.R., 2008. On using carbon and oxygen isotope data from glendonites as paleoenvironmental proxies; a case study from the Permian system of eastern Australia. J. Sediment. Res. 78, 713–723.
Glasspool, I.J., 2000a. Megaspores from the Late Permian lower Whybrow coal seam, Sydney Basin, Australia. Rev. Palaeobot. Palynol. 110, 209–227.
Glasspool, I., 2000b. A major fire event recorded in the mesofossils and petrology of the Late Permian, lower Whybrow coal seam, Sydney Basin, Australia. Palaeogeogr. Palaeoclimatol. Palaeoecol. 164, 357–380.
Glasspool, I.J., 2003. A review of Permian Gondwana megaspores, with particular emphasis on material collected from coals of the Witbank Basin of South Africa and the Sydney Basin of Australia. Rev. Palaeobot. Palynol. 124, 227–296.
Glenister, B.F., Furnish, W.M., 1961. The Permian ammonoids of Australia. J. Paleontol. 35, 673–736.
Golubev, V.K., 2005. Permian tetrapod stratigraphy. In: Lucas, S.G., Ziegler, K.E. (Eds.), The Non-marine Permian. New Mexico: Mus. Nat. Hist Sci. Bull., 30, pp. 95–99.
Gradstein, F.M., Ogg, J.G., Smith, A.G., 2004. A Geologic Time Scale 2004. Cambridge University Press, Cambridge.
Grebe, H., 1970. Permian plant microfossils from the Newcastle Coal Measures/ Narrabeen Group boundary, Lake Munmorah, New South Wales. Geol. Surv. NSW Rec. 12, 125–136.
Greenwood, D.R., Wing, S.L., 1995. Eocene continental climates and latitudinal temperature gradients. Geology 23, 1044–1048.
Grevenitz, P., Carr, P., Hutton, A., 2003. Origin, alteration and geochemical correlation of Late Permian airfall tuffs in coal measures, Sydney Basin, Australia. Int. J. Coal Geol. 55, 27–46.
Gulson, B.L., Diessel, C.F.K., Mason, D.R., Krogh, T.E., 1990. High precision radiometric ages from the northern Sydney Basin and their implication for the Permian time interval and sedimentation rates. Aust. J. Earth Sci. 37, 459–469.
Hales, B., Karp-Boss, L., Perlin, A., Wheeler, P.A., 2006. Oxygen production and carbon sequestration in an upwelling coastal margin. Global Biogeochem. Cycles 20, GB3001.
Hallam, A., Wignall, P.B., 1997. Mass Extinctions and Their Aftermath. Oxford University Press, New York. 320 p.
Hamer, J.M.M., Sheldon, N.D., Nichols, G.J., 2007a. Global aridity during the Early Miocene? A terrestrial paleoclimate record from the Ebro Basin, Spain. J. Geol. 115, 601–608.
Hamer, J.M.M., Sheldon, N.D., Nichols, G.J., Collinson, M.E., 2007b. Late Oligocene–Early Miocene palaeosols of distal fluvial systems, Ebro Basin, Spain. Palaeogeogr. Palaeoclimatol. Palaeoecol. 247, 220–235.
Haworth, M., Gallagher, A., Elliott-Kingston, C., Raschi, A., Marandola, D., McElwain, J.C., 2010. Stomatal index responses of *Agrostis canina* to CO_2 and sulphur dioxide: implications for palaeo-[CO_2] using the stomatal proxy. New Phytol. doi:10.1111/j.1469-8137.2010.03404.x.
Helby, R., 1973. Review of late Permian and Triassic palynology of New South Wales. In: Playford, G.E. (Ed.), Mesozoic and Cainozoic Palynology; Essays in Honour of Isabel Cookson: Geol. Soc. Australia Spec. Publ., 4, pp. 141–147.
Henderson, C.M., 2005. International correlation of the marine Permian time scale. In: Lucas, S.G., Ziegler, K.E. (Eds.), The Non-marine Permian. New Mexico: Mus. Nat. Hist. Sci. Bull., 30, pp. 104–105.

Herbert, C., 1997a. Relative sea level control of deposition in the Late Permian Newcastle Coal Measures of the Sydney Basin, Australia. Sediment. Geol. 107, 167–187.

Herbert, C., 1997b. Sequence stratigraphic analysis of Early and Middle Triassic alluvial and estuarine facies in the Sydney Basin, Australia. Aust. J. Earth Sci. 44, 125–143.

Hermsen, E.J., Taylor, E.L., Taylor, T.N., 2009. Morphology and ecology of the *Antarcticycas* plant. Rev. Palaeobot. Palynol. 153, 108–123.

Huey, R.B., Ward, P.D., 2005. Hypoxia, global warming, and terrestrial Late Permian extinctions. Science 308, 398–401.

Hutchinson, P., 1973. *Pseudobeaconia*, a perleidiform fish from the Triassic Santa Clara Formation, Argentina. Breviora 398, 1–24.

Irving, E., Parry, L.G., 1963. The magnetism of some Permian rocks from New South Wales. Geophys. J. 7, 392–411.

Jahren, A.H., Arens, N.C., 2009. Prediction of atmospheric $\delta^{13}CO_2$ using plant cuticle isolated from fluvial sediment; tests across a gradient in salt content:. Palaios 24, 394–401.

Jahren, A.H., Arens, N.C., Sarmiento, G., Guerrero, J., Amundson, R., 2001. Terrestrial record of methane hydrate dissociation in the Early Cretaceous. Geology 29, 159–162.

Jin, Y.-G., Wang, Y., Sheng, Q., Cao, C.-Q., Erwin, D.H., 2001. Pattern of marine mass extinction across the Permian–Triassic boundary in south China. Science 289, 432–436.

Jubb, R.A., Gardiner, B.G., 1975. A preliminary catalogue of identifiable fossil fish material from southern Africa. S. Afr. Mus. Ann. 67, 1–59.

Knoll, A.H., Bambach, R.K., Payne, J.L., Pruss, S., Fischer, W.W., 2007. Paleophysiology and end-Permian mass extinction. Earth Planet. Sci. Lett. 256, 295–313.

Knutson, T.R., Sirutis, J.J., Garner, S.T., Vecchi, G.A., Held, I.M., 2008. Simulated reduction in Atlantic hurricane frequency under twenty-first-century warming conditions. Nat. Geosci. 1, 359–364.

Konecki, M.C., 1953. Report on the western flank of the Muswellbrook Anticline. Bur. Miner. Resour. Geol. Geophys. Canberra Rec. 133, 1–13.

Kramer, W., Weatherall, G., Offler, R., 2001. Origin and correlation of tuffs in the Permian Newcastle and Wollombi Coal Measures, NSW, Australia, using chemical fingerprinting. Int. J. Coal Geol. 47, 115–135.

Krull, E.S., Retallack, G.J., 2000. $\delta^{13}C$ depth profiles from paleosols across the Permian–Triassic boundary in Antarctica: evidence for methane release. Geol. Soc. Am. Bull. 112, 1459–1472.

Lehrmann, D.J., Ramezani, J., Bowring, S.A., Martin, M.W., Montgomery, P., Enos, P., Payne, J.L., Orchard, M.J., Wang, H., Wei, J., 2006. Timing of recovery from the end-Permian extinction: geochronologic and biostratigraphic constraints from south China. Geology 34, 1053–1056.

Leonova, T.B., 2007. Correlation of the Kazanian of the Volga–Urals with the Roadian of the global Permian scale. Palaeoworld 16, 246–253.

Leonova, T.B., Bogolovskaya, M.F., 1990. Fossil cephalopods: evolutionary trends and systematics of some groups. Tr. Paleontol. Nauka S.S.S.R. 243, 87–97.

Levin, I., Bösinger, R., Bonani, G., Francey, R.J., Kromer, B., Münnick, K.O., Suter, M., Trivett, N.B.A., Wölffi, W., 1992. Radiocarbon in atmospheric carbon dioxide and methane: global distribution and trends. In: Taylor, R.E., Long, A., Kra, R.S. (Eds.), Radiocarbon After Four Decades: An Interdisciplinary Perspective. Springer, New York, pp. 503–518.

Long, J.A., 1998. Dinosaurs of Australia and New Zealand and Other Animals of the Mesozoic Era. Harvard University Press, Cambridge.

Losovsky, V.R., 1998. The Permian–Triassic boundary in the continental series of Eurasia. Palaeogeogr. Palaeoclimatol. Palaeoecol. 143, 273–283.

Loughnan, F.C., 1991. Permian climate of the Sydney Basin — cold or hot? J. Proc. R. Soc. NSW 124, 35–40.

Lucas, S.G., 2009. Timing and magnitude of tetrapod extinctions across the Permo-Triassic boundary. J. Asian Earth Sci. 36, 491–502.

Markwick, P.J., 1994. 'Equability', continentality, and Tertiary 'climate'; the crocodilian perspective. Geology 22, 613–616.

Mauseth, J.D., 2004. Giant shoot apical meristems in cacti have ordinary leaf primordia but altered phyllotaxy and shoot diameter. Ann. Bot. 94, 145–153.

Mayne, S.J., Nicholas, E., Bigg-Wither, A.L., Rasidi, J.S., Raine, M.J., 1974. Geology of the Sydney Basin — a review. Bur. Miner. Resour. Geol. Geophys. Canberra Bull. 149, 1–229.

McMinn, A., 1985. Palynostratigraphy of the Middle Permian coal sequences of the Sydney Basin. Aust. J. Earth Sci. 32, 301–309.

McRae, C., 1999. Life Etched in Stone: Fossils of South Africa. Geological Survey of South Africa, Johannesburg.

Metcalfe, I., Nicoll, R.S., Willink, R.J., 2008. Conodonts from the Permian–Triassic transition in Australia and position of the Permian–Triassic boundary. Aust. J. Earth Sci. 55, 365–377.

Meyer, K.M., Kump, L.R., Ridgwell, A., 2008. Biogeochemical controls on photic-zone euxinia during the end-Permian mass extinction. Geology 36, 747–750.

Mitchell, J., 1924. A preliminary reference to a new species of *Elonichthys* from the lower beds of the Newcastle Coal measures. Linn. Soc. NSW Proc. 49, 503–504.

Mitchell, J., 1925. On *Elonichthys davidi*, in occasional descriptions of N.S.W. Permian fossils. Linn. Soc. NSW Proc. 50, 435–437.

Morante, R., 1996. Permian and early Triassic isotopic records of carbon and strontium in Australia and a scenario of events about the Permian–Triassic boundary. Hist. Biol. 11, 289–310.

Mundil, R., Ludwig, K.R., Metcalfe, I., Renne, P.R., 2004. Age and timing of the Permian mass extinctions: U/Pb dating of closed-system zircons. Science 305, 1760–1763.

Naing, T., 1990. Paleoenvironmental studies of the Middle Triassic uppermost Narrabeen Group, Sydney Basin: paleoecological constraints with particular emphasis on trace fossil assemblages. Unpub.PhD thesis, Macquarie University, 630 pp.

Ovtcharova, M., Bucher, H., Schaltegger, U., Galfetti, T., Brayard, A., Guex, J., 2006. New Early to Middle Triassic U–Pb ages from South China: calibration with ammonoid biochronozones and implications for the timing of Triassic biotic recovery. Earth Planet. Sci. Lett. 243, 463–475.

Payne, J.L., Lehrmann, D.J., Wei, J.-Y., Orchard, M.J., Schrag, D.P., Knoll, A.H., 2004. Large perturbations of the carbon cycle during recovery from the end-Permian extinction. Science 305, 506–509.

Pepperell, J., Grigg, G., 1974. A labyrinthodont trackway from the mid-Triassic near Sydney, New South Wales. Linn. Soc. NSW Proc. 99, 54–56.

Philip, R.P., Saxby, J.D., 1979. Organic geochemistry of coal macerals from the Sydney Basin (Australia). In: Douglas, A.G., Maxwell, J.R. (Eds.), Advances in Organic Geochemistry. Pergamon, Oxford, pp. 639–651.

Popov, A.V., 2005. A new species of *Epijuresanites* (Ammonoidea) from the Permian of Pai-Khoi. Paleontol. J. 39, 17–18.

Pruss, S.B., Bottjer, D.J., 2004. Late Early Triassic microbial reefs of the western United States; a description and model for their deposition in the aftermath of the end-Permian mass extinction. Palaeogeogr. Palaeoclimatol. Palaeoecol. 211, 127–137.

Raam, A., 1969. Gerringong volcanics. In: Packham, G.H. (Ed.), The Geology of New South Wales: Geol. Soc. Australia J., 16, pp. 366–368.

Retallack, G.J., 1975. The life and times of a Triassic lycopod. Alcheringa 1, 3–29.

Retallack, G.J., 1980. Late Carboniferous to Middle Triassic megafossil floras from the Sydney Basin. In: Helby, R., Herbert, C. (Eds.), Geology of the Sydney Basin: Geol Surv. N.S.W. Bull., 26, pp. 384–430.

Retallack, G.J., 1995. Permian–Triassic life crisis on land. Science 267, 77–80.

Retallack, G.J., 1996. Early Triassic therapsid footprints from the Sydney Basin, Australia. Alcheringa 20, 301–314.

Retallack, G.J., 1997a. Earliest Triassic origin of *Isoetes* and quillwort evolutionary radiation. J. Paleontol. 71, 500–521.

Retallack, G.J., 1997b. Palaeosols in the upper Narrabeen Group of New South Wales as evidence of Early Triassic palaeoenvironments without exact modern analogues. Aust. J. Earth Sci. 44, 185–201.

Retallack, G.J., 1998. Fossil soils and completeness of the rock and fossil records. In: Donovan, S.K., Paul, C.R.C. (Eds.), The Adequacy of the Fossil Record. Wiley, Chichester, pp. 133–153.

Retallack, G.J., 1999a. Permafrost palaeoclimate of Permian palaeosols in the Gerringong volcanic facies of New South Wales. Aust. J. Earth Sci. 46, 11–22.

Retallack, G.J., 1999b. Postapocalyptic greenhouse paleoclimate revealed by earliest Triassic paleosols in the Sydney Basin, Australia. Geol. Soc. Am. Bull. 111, 52–70.

Retallack, G.J., 2001a. A 300 million year record of atmospheric carbon dioxide from fossil plant cuticles. Nature 411, 287–290.

Retallack, G.J., 2001b. Soils of the Past. Blackwell, Oxford.

Retallack, G.J., 2002. *Lepidopteris callipteroides*, an earliest Triassic seed fern of the Sydney Basin, southeastern Australia. Alcheringa 26, 475–500.

Retallack, G.J., 2005a. Earliest Triassic claystone breccias and soil-erosion crisis. J. Sediment. Res. 75, 679–695.

Retallack, G.J., 2005b. Permian greenhouse crises. In: Lucas, S.G., Ziegler, K.E. (Eds.), The Nonmarine Permian: Bull. New Mexico Mus. Nat. Hist. Sci., 30, pp. 256–269.

Retallack, G.J., 2008. Warm-spike or cool-climate lateritic bauxites at high latitudes? J. Geol. 116, 558–570.

Retallack, G.J., 2009. Mesozoic greenhouse crises. Geol. Soc. Am. Bull. 121, 1441–1445.

Retallack, G.J., Jahren, A.H., 2008. Methane release from igneous intrusion of coal during Late Permian extinction events. J. Geol. 116, 1–20.

Retallack, G.J., Krull, E.S., 2006. Carbon isotopic evidence for terminal-Permian methane outbursts and their role in extinctions of animals, plants, coral reefs and peat swamps. In: Greb, S., DiMichele, W.A. (Eds.), Wetlands through Time: Geol. Soc. Amer. Spec. Pap., 399, pp. 249–268.

Retallack, G.J., Veevers, J.J., Morante, R., 1996. Global early Triassic coal gap between Late Permian extinction and Middle Triassic recovery of peat-forming plants. Geol. Soc. Am. Bull. 108, 195–207.

Retallack, G.J., Smith, R.M.H., Ward, P.D., 2003. Vertebrate extinction across the Permian–Triassic boundary in the Karoo Basin of South Africa. Geol. Soc. Am. Bull. 115, 1133–1152.

Retallack, G.J., Metzger, C.A., Greaver, T., Jahren, A.H., Sheldon, N.D., Smith, R.M.H., 2006. Middle–Late Permian mass extinction on land. Geol. Soc. Am. Bull. 118, 1398–1411.

Revelle, R.R., Suess, H.E., 1957. Carbon dioxide exchange between atmosphere and ocean and the question of an increase of atmospheric CO_2 during the past decades:. Tellus 9, 18–27.

Riccardi, A., Kump, L.R., Arthur, M.A., d'Hondt, S., 2007. Carbon isotopic evidence for chemocline upward excursions during the end-Permian event. Palaeogeogr. Palaeoclimatol. Palaeoecol. 248, 73–81.

Rich, T.H.V., Vickers-Rich, P., 2000. Dinosaurs of Darkness. Indiana University Press, Bloomington.

Richoz, S., 2006. Stratigraphie et variations isotopiques du carbone dans le Permien supérieur et les Trias inférieur de quelques localités de la Néotéthys (Turquie, Oman et Iran). Memoires de Géologie Lausanne 46, 1–275.

Rigby, J.F., 1964. The Lower Gondwana flora of the Illawarra Coal Measures, Wollongong, New South Wales, Australia. Section 9 Gondwana Int. Geol. Cong. 22, India, Proc. 9, 3–25.

Rigby, J.F., 1966. Some Lower Gondwana articulates from New South Wales. In: Sahni, S. (Ed.), Symposium on Floristics and Stratigraphy of Gondwanaland. Birbal Sahni Institute of Palaeobotany, Lucknow, pp. 48–54.

Rigby, J.F., 1967. On *Gangamopteris walkomii* sp. nov. Aust. Mus. Rec. 27, 175–182.

Rigby, J.F., 1969. *Cordaicladus adamsii* (Feistmantel) Rigby comb. nov. Linn. Soc. NSW Proc. 94, 52–54.

Roberts, J., Claoue-Long, J.C., Foster, C.B., 1996. SHRIMP zircon dating of the Permian System of eastern Australia. Aust. J. Earth Sci. 43, 401–421.

Royer, D.L., Osborne, C.P., Beerling, D.J., 2002. High CO_2 increases the freezing sensitivity of plants; implications for paleoclimatic reconstructions from fossil floras. Geology 30, 963–966.
Royer, D.L., Berner, R.A., Montañez, I., Beerling, D.J., 2004. CO_2 as a primary driver of Phanerozoic climate. GSA Today 14, 4–10.
Sakai, A., Larcher, W., 1987. Frost Survival of Plants. Springer, Berlin.
Schaeffer, B., Mangus, M., 1976. An Early Triassic fish assemblage from British Columbia. Am. Mus. Nat. Hist. Bull. 156, 515–564.
Schiappa, T.A., Hemmesch, N.T., Spinosa, C., Nassichuk, W.W., 2005. Cisuralian ammonoid genus *Uraloceras* in North America. J. Paleontol. 79, 366–377.
Schultze, H.-P., Kriwet, J., 1999. Die Fische der Germanischen Trias. In: Hauschke, N., Wilde, V. (Eds.), Trias: eine Ganz andere Welt. Pfeil, München, pp. 239–250.
Scotese, C.R., 1997. Platetracker for Windows (Computer Program). Paleomap, Arlington, Texas.
Selleck, B.W., Carr, P.F., Jones, B.G., 2007. A review and synthesis of glendonites (pseudomorphs after ikaite) with new data: assessing applicability as recorders of ancient coldwater conditions. J. Sediment. Res. 77, 908–991.
Shaw, A.B., 1964. Time in Stratigraphy. McGraw Hill, New York.
Sheldon, N.D., 2006. Abrupt chemical weathering increase across the Permian–Triassic boundary. Palaeogeogr. Palaeoclimatol. Palaeoecol. 231, 315–321.
Sheldon, N.D., Retallack, G.J., 2002. Low oxygen levels in earliest Triassic soils. Geology 30, 919–922.
Sheldon, N.D., Tabor, N.J., 2009. Quantitative paleoenvironmental and paleoclimatic reconstruction using paleosols. Earth Sci. Rev. 95, 1–95.
Sheldon, N.D., Retallack, G.J., Tanaka, S., 2002. Geochemical climofunctions from North American soils, and application to paleosols across the Eocene–Oligocene boundary. J. Geol. 110, 687–696.
Sigman, D.M., Boyle, E.A., 2000. Glacial/interglacial variations in atmospheric carbon dioxide. Nature 407, 859–869.
Song, H.-J., Tong, J.-N., Chen, Z.-Q., Yang, H., Wang, Y.-B., 2009. End-Permian mass extinction of foraminifers in the Nanpanjiang Basin, south China. J. Paleontol. 83, 718–738.
Steiner, M.B., 2006. The magnetic polarity time scale across the Permian–Triassic boundary. In: Lucas, S.G., Cassinis, G., Schneider, J.W. (Eds.), Non-marine Permian Biostratigraphy and Biochronology: Geol. Soc. London Spec. Publ., 265, pp. 15–38.
Tabor, N.J., Montanez, I.P., Steiner, M.B., Schwindt, D., 2007. $\delta^{13}C$ values of carbonate nodules across the Permian–Triassic boundary in the Karoo Supergroup (South Africa) reflect a stinking sulfurous swamp, not atmospheric CO_2. Palaeogeogr. Palaeoclimatol. Palaeoecol. 252, 370–381.
Tanner, L.H., Smith, D.L., Allan, A., 2007. Stomatal response of swordfern to volcanogenic CO_2 and SO_2 from Kilauea Volcano. Geophys. Res. Lett. 34, L15807. doi:10.1029/2007 GL030320, 2007.
Theveniaut, H., Klootwijk, C., Foster, C., Giddlings, J., 1994. Revisiting the "Kiaman"; defining the boundaries of the PCRS in the Hunter Valley and Sydney Basin, Australia. Eos 75, 203.
Tong, J., Zhou, X., Erwin, D.H., Zuo, J., Zhao, L., 2006. Fossil fishes from the Lower Triassic of Majiashan, Chaohu, Anhui Province, China. J. Paleontol. 80, 146–161.
Townrow, J.A., 1968. A fossil *Selaginella* from the Permian of New South Wales. Linn. Soc. Bot. J. 61, 13–23.
Trewartha, G.T., 1982. Earth's Problem Climates. Univ. Wisconsin Press, Madison.
Twitchett, R.J., 2007. The Lilliput effect in the aftermath of the end-Permian extinction. Palaeogeogr. Palaeoclimatol. Palaeoecol. 252, 132–144.
Visscher, H., Looy, C.V., Collinson, M.E., Brinkhuis, H., van Konijnenburg-van Cittert, J.H.A., Kürschner, W.M., Sephton, M.A., 2004. Environmental mutagenesis during the end-Permian ecological crisis. Proc. Nat. Acad. Sci. U.S.A. 101, 12952–12956.
Wade, R.T., 1935. Triassic Fishes of Brookvale, New South Wales. British Museum of Natural History, London.
Wang, W., Cao, C., Wang, Y., 2004. The carbon isotope excursion on GSSP candidate section of Lopingian–Guadalupian boundary. Earth Planet. Sci. Lett. 220, 57–67.
Walkom, A.B., 1928. Notes on some additions to the Glossopteris flora in New South Wales. Linn. Soc. NSW Proc. 53, 555–564.
Walkom, A.B., 1941. On a new species of *Annularia* from New South Wales. Aust. Mus. Rec. 21, 43–44.
Weidlich, O., 2007. PTB mass extinction and earliest Triassic recovery overlooked? New evidence for a marine origin of Lower Triassic mixed carbonate siliciclastic sediments (Rogenstein Member), Germany. Palaeogeogr. Palaeoclimatol. Palaeoecol. 252, 259–269.
Welles, S.P., Cosgriff, J., 1965. A revision of the labyrinthodont family Capitosauridae, and a description of *Parotosaurus peabodyi* n. sp., from the Wupatki Member of the Moenkopi Formation of Arizona. Univ. Calif. Publ. Geol. Sci. 54, 1–148.
White, M.E., 1986. The Greening of Gondwana. Reed, Balgowlah.
Wignall, P.B., Sun, Y.-D., Bond, D.P.G., Izon, G., Newton, R.J., Vedrine, S., Widdowson, M., Ali, J.R., Lai, L.-L., Jiang, H.S., Cope, H., Bottrell, S.H., 2009. Volcanism, mass extinction and carbon isotope fluctuations in the Permian of China. Science 324, 1179–1182.
Woodward, A.S., 1890. The fossil fishes of the Hawkesbury Series at Gosford. Geol. Surv. NSW Palaeontol. Mem. 4, 1–55.
Woodward, A.S., 1908. The fossil fishes of the Hawkesbury Series at St Peters. Geol. Surv. NSW Palaeontol. Mem. 10, 1–29.
Woodward, A.S., 1931. On *Urosthenes*, a fossil fish from the upper Coal measures of Lithgow, New South Wales. Ann. Mag. Nat. Hist. 8, 365–367.
Wynn, J.G., 2007. Carbon isotope fractionation during decomposition of organic matter in soils and paleosols; implications for paleoecological interpretations of paleosols. Palaeogeogr. Palaeoclimatol. Palaeoecol. 251, 437–448.